

Review

UV Spectroscopy of Massive Stars

D. John Hillier

Department of Physics and Astronomy & Pittsburgh Particle Physics, Astrophysics and Cosmology Center (PITT PACC), University of Pittsburgh, 3941 O'Hara Street, Pittsburgh, PA 15260, USA; hillier@pitt.edu

Received: 11 July 2020; Accepted: 6 August 2020; Published: 12 August 2020



Abstract: We present a review of UV observations of massive stars and their analysis. We discuss O stars, luminous blue variables, and Wolf–Rayet stars. Because of their effective temperature, the UV (912 – 3200 Å) provides invaluable diagnostics not available at other wavebands. Enormous progress has been made in interpreting and analysing UV data, but much work remains. To facilitate the review, we provide a brief discussion on the structure of stellar winds, and on the different techniques used to model and interpret UV spectra. We discuss several important results that have arisen from UV studies including weak-wind stars and the importance of clumping and porosity. We also discuss errors in determining wind terminal velocities and mass-loss rates.

Keywords: massive stars; O stars; Wolf–Rayet stars; UV; mass loss; stellar winds

1. Introduction

According to Wien's Law, the peak of a star's energy distribution occurs in the UV for a star whose temperature exceeds 10,000 K. In practice, the temperature needs to exceed 10,000 K because of the presence of the Balmer jump. Temperatures greater than 10,000 K correspond to main-sequence stars of mass greater than $\sim 2 M_{\odot}$ and spectral types B9 and earlier.

Early UV observations were made by rocket-flown instruments (e.g., [1,2]). Observations of six OB supergiants in Orion revealed prominent emission lines due to Si IV $\lambda\lambda 1394, 1403$ and C IV $\lambda\lambda 1548, 1552$. These emission lines also exhibited prominent absorption lines blueshifted by $\sim 2000 \text{ km s}^{-1}$, signifying that the giants and supergiants were losing mass in a stellar wind [2]. Spectral lines exhibiting both emission and blueshifted absorption are classified as P Cgyni profiles ([3] and Figure 1). However, it was the advent of the satellites Copernicus (launched in 1972) and, in particular, the International Ultraviolet Explorer (IUE; launched in 1978) that greatly expanded our knowledge about the UV spectra of massive stars.

The importance of the UV is severalfold. First it contains many resonance lines (e.g., C III $\lambda 977$, C IV $\lambda\lambda 1548, 1552$, Si IV $\lambda\lambda 1394, 1403$, N V $\lambda\lambda 1238, 1242$, O VI $\lambda\lambda 1031, 1038$, P V $\lambda\lambda 1118, 1128$), important intercombination lines (C III] $\lambda 1909$, N IV] $\lambda 1486$), and subordinate lines (C III $\lambda 2297$, N IV $\lambda 1719$, O V $\lambda 1371$, S V $\lambda 1501$). The resonance lines are particularly useful as they are sensitive to lower mass-loss rates than $H\alpha$, and provide measures of the outflow speed. In B stars numerous other resonance transitions are also visible (C II, Mg II, Al III, P IV). The UV is also rich in iron lines—Fe II and Fe III are prominent in B stars while in hotter stars we see Fe IV to Fe VII.

In B stars it is possible to measure (albeit after allowance for reddening) the bolometric luminosity directly. In general, the line spectrum is richer at wavelengths below the spectral maximum. For cooler massive stars, the observable UV allows the direct detection of the lines responsible for driving the stellar wind. To date this property of the UV has not been well exploited.

Stars with an initial mass of greater than $\sim 8 M_{\odot}$ (i.e., earlier than B2V) end their life either as a core collapse supernova (SN), a pair instability SN, or collapse directly to a black hole, and for simplicity we will confine this review to these stars. The evolution of a massive star is quite complicated (e.g., [4]).

Stars less massive than $\approx 20 M_{\odot}$ evolve to the right on the Hertzsprung-Russell (HR) diagram where they exist as red supergiants (RSGs) before they explode as a Type IIP core collapse SN (e.g., [5]). The evolution of stars between $20 M_{\odot}$ and $30 M_{\odot}$ is uncertain and controversial. These stars may explode as a Type IIP SN but there is a lack of observational evidence to confirm this (see, e.g., [6]), and there is considerable debate whether the absence of Type IIP progenitors with a mass greater than $20 M_{\odot}$ is real, or simply an artifact of low number statistics (see, e.g., [7]). Further, due to uncertainties in stellar evolution, it has been argued that it is impossible to infer the progenitor mass from the properties of the progenitor at the time of the explosion [8]. Likewise, it is difficult to estimate the progenitor mass from modelling of the light curve [9]. Some stars may explode as a different class of SN (e.g., IIb), while others may simply collapse directly to a black hole. Due to quirks of stellar evolution some progenitor masses are less likely to explode than others, and the likelihood of explosion is not a simple function of mass (e.g., [10,11]).

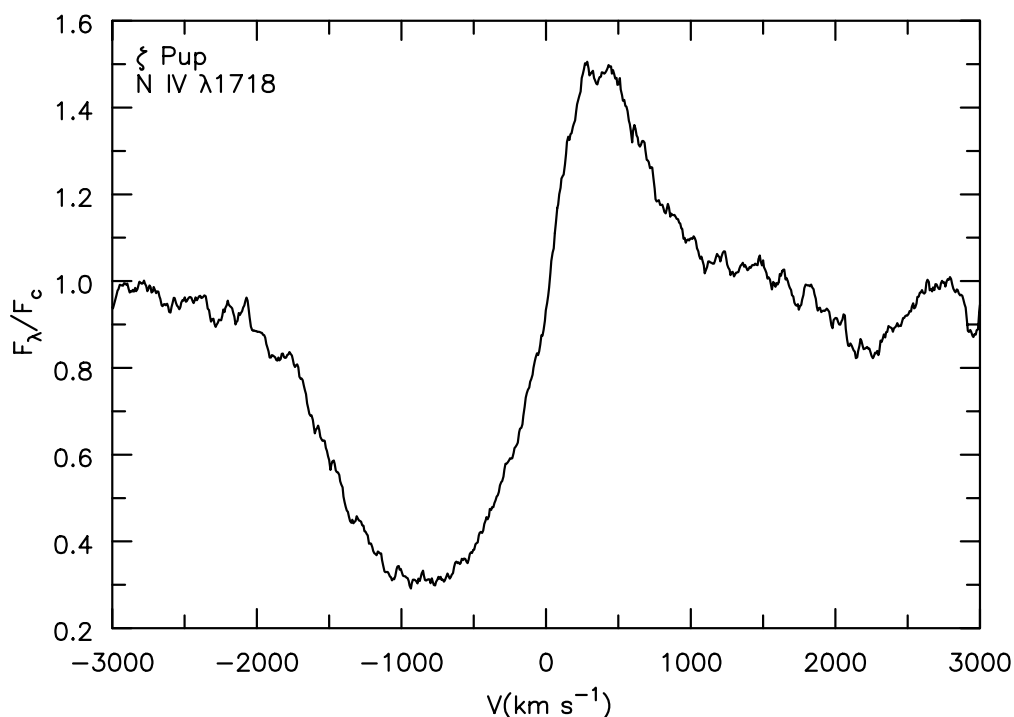


Figure 1. The N IV $\lambda 1718$ transition in ζ Puppis (O4I(n)fp) showing a classic P Cygni profile.

In our Galaxy, stars more massive than $30 M_{\odot}$ probably never evolve to become a RSG—rather they evolve through several other phases such as a blue supergiant (BSG), yellow supergiant (YSG), luminous blue variable (LBV), or Wolf–Rayet (WR) star (see, e.g., [12] and references therein). BSGs and YSGs are simply evolved massive stars at cooler temperatures that could be evolving to the left or right in the HR diagram. Like O stars they are undergoing mass loss, and many exhibit variability in the UV. WR stars exhibit numerous optical emission lines, and typically show evidence for enrichment of the atmosphere by CNO-processed material (the WN classes) or helium burning (WC and WO sub-classes). The classification of WR stars is primarily based on their ionisation, with lower numbers (e.g., 3 in WN3) exhibiting higher ionisation [13]. The properties of WC stars (e.g., terminal velocity) generally correlate strongly with their spectral class [14], while the WN class is very heterogeneous (e.g., [15]). To remove some of the heterogeneity, WN stars with hydrogen are designated as WNh. While many WR stars are significantly evolved (e.g., core helium burning), some of the most massive WNh stars may still be core hydrogen burning (e.g., [16,17]). These massive stars show strong emission lines in their optical spectra because of their high luminosities. However, they still show evidence of the CNO-processed material in the photosphere (e.g., enhanced He and N) (e.g., [18,19]).

The final fate of the most massive stars is even more uncertain. While some do explode as a spectacular SN, others may simply collapse to form a black hole. However mass may be ejected even when a black hole forms (e.g., [20]). It has typically been assumed that Ibc SNe are commonly associated with the collapse of massive stars, but their ejecta masses (e.g., [21–23]) and statistical arguments, based on the initial mass function and frequency of binary systems, suggest that many of them are more likely associated with lower mass progenitors that have undergone mass exchange in a binary system (e.g., [24]). There is evidence that Type Ic SNe (i.e., SNe that lack the strong Si II lines of Type Ia SNe, and show no evidence for He or H lines in their optical spectrum [25]) come from higher mass stars than do Type Ib (similar to Type Ic but show evidence for He in the optical spectrum) and Type II SNe (e.g., [26]). The broad-lined Type Ic SNe and long-duration gamma-ray bursts are likely to be associated with massive stars (e.g., [27] and references therein).

This review primarily discusses the UV. In practice, today’s analyses are best done using a wide wavelength coverage—from X-rays to radio. Different spectral regions contain different diagnostics and, importantly, provide consistency checks for results from other regions. We will also ignore the interstellar medium (ISM)—the UV of O stars provides a convenient background to study the ISM in, for example, our galaxy, and the Magellanic Clouds. There are several previous reviews that cover the UV (e.g., [28,29]). Obviously there will be some overlap with the current review. There are also extensive reviews on massive stars [30–32].

In this review we will highlight some key results for which the UV has been an important diagnostic. For reasons of space the review is necessarily incomplete, and any omission is not a reflection on the quality or importance of the work. For reasons of brevity we will often speak in general terms without discussing the exceptions. Occasionally we will talk of some property as belonging to a particular class of star, but in general properties are continuous. The review is organised as follows: We discuss some of the atlases that are available for O stars (Section 2.1) and WR stars (Section 2.2). To facilitate later discussion we provide a brief overview of the structure of non-magnetic hot star winds in Section 3. In Section 4 we discuss the modelling of UV spectra highlighting the two fundamental approaches—modelling of individual wind lines (or doublets), and full spectral synthesis. In this section we also briefly discuss modelling the influence of stellar rotation on spectra (Section 4.2), and modelling spectra of binary systems (Section 4.3). Next, in Section 5, we provide a detailed discussion of some of the key results that have arisen from UV studies of (primarily) O stars. These include: the importance of the UV for mass-loss determinations (Section 5.1), observations of the extreme ultraviolet (Section 5.2), weak winds (Section 5.3), superions¹ (Section 5.4), non Galactic/Magellanic studies (Section 5.5), and the iron forest (Section 5.6). We then briefly discuss UV observations and models for other classes of massive stars: WR stars (Section 6.1), the magnetic O stars (Section 6.2) and LBVs (Section 6.3). Finally we discuss accuracies in V_{∞} (Section 7.1) and mass-loss rates measured from UV spectra (Section 7.2).

2. Spectral Atlases

As often discussed by Nolan Walborn, morphological studies of spectra can reveal systematic trends and potentially reveal new classes of stars, and such trends and relationships must be understood if we are to understand massive stars (e.g., [33]). For morphological studies, spectral atlases are important, and many UV atlases exist. Below we first discuss atlases for OB stars, then atlases for WR stars.

2.1. OB Stars

As noted earlier, the first UV spectra for B stars came from rocket-flown instruments [2]. The next major advance came with the Copernicus satellite which covered the UV spectral ranges 900–1560 Å and 1650–3150 Å. Selected line profiles were presented by [34] while [35] presented an atlas/catalog of spectra from 1000 to 1450 Å at 0.2 Å resolution. Later, [36] presented a UV atlas of OB spectra extending

¹ Early observations showed the existence of a strong O VI $\lambda\lambda 1031, 1038$ P Cygni profile in many O stars. Since the effective temperature of the star is too low to produce appreciable O⁵⁺, O⁵⁺ is termed a superion.

from 1000 to 1200 Å. IUE atlases, with a constant spectral resolution of 0.25 Å, for both OB stars and B stars were presented by [37,38]. Later a UV spectral atlas of 25 O3-B8 supergiants, also with a spectral resolution of 0.25 Å, was presented by [39]. These works discuss spectral morphologies and trends, and the behaviours of wind lines of species with widely different ionisation potentials.

The availability of spectral data on massive stars between the Lyman limit and 1200 Å was greatly expanded by the Far Ultraviolet Spectroscopic Explorer (FUSE) telescope. Spectral atlases for stars in the Galaxy ($\Delta\lambda = 0.12$ Å; [40]) and Magellanic Clouds ($\Delta\lambda = 0.25$ Å; [41]) were published. The Magellanic Clouds atlas is particularly useful—shortward of 1200 Å, interstellar lines due to H I and H₂ strongly influence the spectrum of reddened stars, a severe problem for most galactic O stars. The FUSE spectral region has many accessible wind lines—Si IV $\lambda\lambda 1122, 1128$, N III $\lambda\lambda 990, 992$, N IV $\lambda 955$, S IV $\lambda\lambda 1063, 1072$, O VI $\lambda\lambda 1031, 1038$ and P V $\lambda\lambda 1118, 1128$ (e.g., [41]). O VI $\lambda\lambda 1031, 1038$ is particularly important as it is in a relatively “clean” spectral region, and O⁵⁺ is regarded as a superior for most O stars (Section 5.4). The P V $\lambda\lambda 1118, 1128$ doublet turned out to be very useful. In many O stars P⁴⁺ is the dominant ionisation stage of P in the wind, and because of its low abundance the P V $\lambda\lambda 1118, 1128$ lines are unsaturated (e.g., [42–44]). They can thus be used to probe mass-loss rates, clumping, and porosity (see Sections 4 and 5.3).

Several Hubble Space Telescope (HST) atlases also exist. For example, an atlas of metal-deficient stars in the SMC was presented by [45]. The winds in these stars are much weaker than in the galaxy, and are thus of interest for studying distant starburst galaxies. An additional atlas is the spectral UV atlas of 10 Lac (O9V) which was obtained with the Goddard High Resolution Spectrograph on the Hubble Space Telescope. This atlas provides line identifications, and covers the region from ~1180 to 1780 Å at a spectral resolution of 15 km s⁻¹ and with a signal-to-noise ratio of greater than 100. This line list complements an earlier data set based on IUE data [46]. The Advanced Spectral Library (ASTRAL) was an HST Treasury Program [47] which obtained high-signal-to-noise (>100) ultraviolet (115–310 nm) observations of a representative sample of nearby bright stars at resolutions ($\lambda/\Delta\lambda$) of 30,000–100,000. Included in this sample were many important O and B stars, including HD 66811 (Zeta Puppis, O4I(n)fp), HD 46223 (O4V(f)), HD 101190 (O6IV(f)), HD 46202 (O9.2V), and HD 52089 (Eps CMa, B1.5II).

2.2. Wolf–Rayet Stars

An extensive atlas of IUE UV spectra of Wolf–Rayet stars, with line identifications, has been provided by [48]. The spectra of some WNh stars (such as HD 92740, WR) are similar to those of O stars except that emission lines are more pronounced. The UV spectra of WNE stars are dominated by emission lines with C IV $\lambda\lambda 1548, 1552$, N IV $\lambda 1486$, N V $\lambda\lambda 1238, 1242$, He II $\lambda 1640$ among the most prominent. The He II $n = 3$ lines are also visible in WN stars. Most of the resonance P Cygni profiles also have a significant thermal component—they do not simply arise by scattering. In WC stars lines such as C IV $\lambda\lambda 1548, 1552$, numerous transitions between the $n = 4$ (i.e., 4s–4f) and $n = 5$ (i.e., 5s–5g) levels in C IV ($\lambda\lambda 2100–2700$), C III $\lambda 2297$ and C III $\lambda 1909$ dominate the UV spectrum. Shortward of 1500 Å, Fe lines form a pseudo continuum.

A Hopkins Ultraviolet Telescope Far-Ultraviolet Spectral atlas [49] and a FUSE spectral atlas [50] cover the wavelength region from 900–1200 Å. The key spectral features in this spectral region are similar to those discussed earlier for O stars. Not surprisingly, wind features are more apparent, and carbon emission lines are much stronger in WC stars.

3. Structure of Hot Star Winds

Radiation-driven winds are inherently unstable (e.g., [51,52]), and this leads to the formation of shocks and clumped winds. While wind instabilities can be self-initiated, it is also possible that they are seeded by sub-surface convection (e.g., [53,54]). Under the assumption that the clumps are optically thin, and that there are many clumps in a photon-mean-free path, the clumping (termed microclumping) is typically characterised by the volume filling factor f defined by $f = \langle \rho \rangle^2 / \langle \rho^2 \rangle$, where ρ is the local mass density, and $\langle \rangle$ denotes a spatial average. The volume filling factor is

also utilised in planetary nebulae studies. In the literature the clumping factor, $D = 1/f$, is also used to characterise the clumping, and the interclump medium is usually neglected. The inclusion of microclumping into radiative transfer codes is relatively easy—we simply use the “clumped” density to evaluate all opacities and emissivities, and then scale these quantities by f (e.g., [55]). The assumption of optically thin clumps is much more realistic for continuum transfer, than for transfer in spectral lines. If the clumps are not optically thin we use the term macroclumping. An effective opacity formalism for a two-component medium has been developed [56]. Two phenomena related to clumping are spatial porosity and porosity in velocity space (hereafter termed vorosity; [57]).

Spatial porosity refers to the escape of photons via regions that are of much lower density (or void) than the mean wind. There is an ongoing debate within the hot-star community as to the importance of porosity for analysing spectra of massive stars [58–61].

Vorosity refers to the absence of material (or of much lower optical depth) at certain discrete velocities, and is seen to arise in radiation hydrodynamic simulations of stellar winds (e.g., [52]). Along a single sight line to the star an observer will see a blueshifted absorption profile that is not continuous—rather it will exhibit discrete absorption components (whose depth will depend on the transition under consideration). In some cases the absorption may extend to zero. When averaged over multiple sight lines striking the star a smooth profile may be obtained, but in general it will not be black (i.e., close to zero). In such cases the column density of ions can be severely underestimated. This is discussed further in Section 7.2.

Clumping manifests itself in several different ways: Firstly, by variability. In the optical it reveals its presence by a variable structure in emission line profiles (e.g., [62–64]). In the UV the variability often manifests by variable discrete absorption components (termed DACs) in unsaturated UV P Cygni profiles (e.g., [65]), and in the extent and shape of the blue edge of P Cygni profiles.

Variability of wind features is ubiquitous, and was readily apparent in Copernicus spectra [66]. Before the demise of IUE in 1996, an extensive observational campaign was undertaken to monitor variability in several early type stars [67]. Extensive observations were made of ζ Puppis (O4I(n)fp) [68], HD 50896 (WN4.5) [69], and HD 64760 (B0.5 Ib) [70]. For HD 64760, the observations showed evidence for co-rotating wind features with a 1.2 d periodicity (factor of four less than the maximum rotation period), and suggest that the variations are rotationally modulated. Observations of ζ Puppis found evidence for two periods—19.2 h and 5.2 days. The first period was related to the occurrence of discrete absorption components (DACs) in the Si IV $\lambda\lambda 1394, 1403$ profile, and indicates no direct relation to surface features. The 5.2 days period was identified as the rotation period. The periodicities found did not match those seen in X-ray and H α data (16.7 h, [71]) or optical absorption lines (8.5 h, [72]).

Observations of HD 50896 (EZ Canis Majoris, WR6) revealed variability with the same 3.76 days period found from optical lines. At various times this has been interpreted as a rotation period, and as an orbital period. The later was always difficult to reconcile with observations over long periods—while the period remained the same, different sets of observations required different phasing. More recently, it has been suggested that the cause of the phase variations is apsidal motion [73], and that HD 50896 is a binary system containing a WR star and a late-type B star of 3 to 5 M_{\odot} [74].

Given our increased understanding and modelling capabilities, these old IUE data sets are a potential goldmine for obtaining further information on the structure of stellar winds.

The second way clumping manifests itself is through inconsistencies in mass-loss rates derived from different diagnostics. In general, mass-loss rates derived from density-squared diagnostics, such as H α emission in O stars and He II recombination lines in WR stars, are higher than mass-loss rates derived from density-dependent diagnostics (unsaturated P Cygni profiles belonging to the dominant ionisation stage in O stars, electron scattering wings in WR stars). An important, and unresolved issue, is how much of the inconsistency is due to density variations², and how much is due to either porosity or vorosity.

² Because of historical precedents, density variations are often referred to as clumping in the literature, and this is often treated/discussed separately from the effects of porosity and vorosity.

The third way, related to X-rays, is the shape of and shifts in X-ray lines. The shape of X-ray profiles will depend on where they originate, and on the background optical depth of the “cool” wind. The latter primarily scales with the wind density. Analysis of X-ray profiles indicates that they originate in the stellar wind (and not a corona) (e.g., [75]), and that the implied mass-loss rate is lower than that derived using density-squared diagnostics at other wavelengths (e.g., [76]). Porosity may also contribute to the escape of X-rays, but a porous wind is also, by necessity, a clumped wind. Of course, the mere existence of X-rays, and their origin within the stellar wind, is by itself an important indicator of the inhomogeneous nature of stellar winds.

A fourth way, discussed in Section 7.2, is through the analysis of UV doublet line profiles.

4. Modelling of the UV Spectra

4.1. Single Stars

Interpreting the UV spectra of O and WR stars is generally quite difficult. Due to numerous bound-bound transitions the continuum is not easily identifiable, and this becomes increasingly true at shorter wavelengths in O stars, and is generally true in WR stars (Figure 2). This is exacerbated by the difficulty of determining an accurate reddening, uncertainties in the reddening law, and variations in the reddening law between galaxies, and within the galaxy itself. For the standard [77] extinction law $A_{1440\text{\AA}}/E_{B-V} = 8.3$, a change of 0.01 in E_{B-V} causes roughly a 10% change in flux. Obviously it is impossible to derive the UV energy distribution to a high degree of accuracy. However, such a fitting is generally done in WR stars because the continuum cannot be identified. In O stars the Fe absorption forest plays a similar role to the Fe emission forest in WR stars. To avoid systematic errors the UV should, ideally, be modelled in conjunction with other spectral regions.

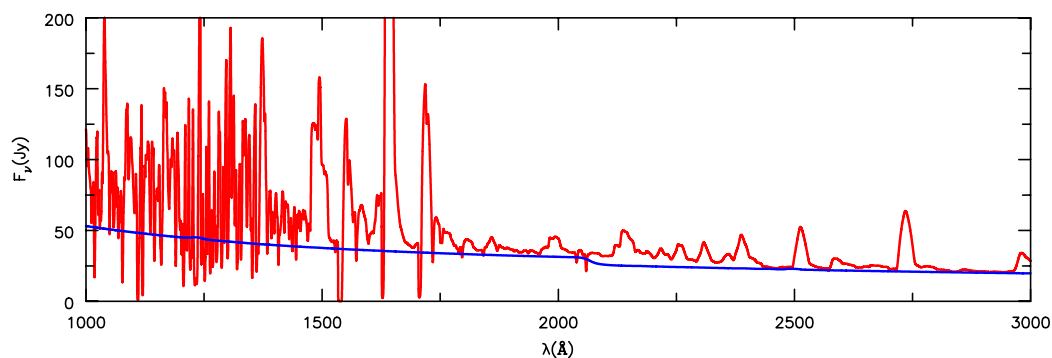


Figure 2. Illustration of the spectrum and continuum for a WNE-type star. Everywhere shortward of 2200 Å, the continuum is masked by lines making it virtually impossible to rectify the spectrum. As a consequence, comparisons are usually done in flux space, but this is difficult due to uncertainties in the reddening. Near 2200 Å in the continuum spectrum we see the series limit for He II(n-3) whose presence in the full spectrum is masked by blending of higher members of the He II(n-3) series. A similar effect occurs for the Pickering/Balmer jump [78]. The four strongest lines in the spectrum are N IV] λ1486, C IV λλ1548, 1552, He II λ1640, and N IV λ1719. The apparent noise between 1000 and 1500 Å is primarily due to Fe lines – they are much more obvious with an expanded scale.

Modelling of UV spectra falls into two classes: modelling of individual UV line profiles (or doublets) and full spectral synthesis. In the first category we highlight the “Sobolev with Exact Integration” (SEI) technique promoted by [79], which was developed using the realisation that while the Sobolev approximation is moderately accurate for computing the line source function, it does a poor job of predicting line profiles (see, e.g., [80]). In the SEI method the velocity law and the optical depth are treated as free parameters, the line-source function is computed using the Sobolev approximation, and the line profile is computed using a formal solution of the transfer equation in the observer’s frame. In addition, it is necessary to specify the photospheric radiation field. Due to the

simplifying assumptions, fitting of line profiles is rapid, and best-fit parameters can be determined. Unfortunately there are many parameters, and there is no check on whether the best-fit parameters are consistent (i.e., can be reproduced) with the star's radiation field. The accuracy of the model parameters very much depends on the type of profiles and the species being modelled. For example, saturated P Cygni profiles are insensitive to the mass-loss rate. Further, the mass-loss rate can only be derived if the abundance is known, and if the ion producing the line is the dominant species in the wind. The SEI method has been used by different groups, has been extended (e.g., [43]), and has produced many important results (Section 5.1).

Monte Carlo (MC) codes have also been used to study the formation of UV resonance line profiles. Their advantage is that they are easily extended to 3D, and can handle (at least in principle) arbitrary density structures. Because of clumping, the Sobolev approximation cannot be used, and the optical depth has to be estimated using a numerical integration. Typically such calculations have generally been restricted to resonance line scattering (e.g., [60,81,82]).

With the exception of wind lines, the UV spectra of O and B stars can, to some extent, be modelled using plane-parallel atmosphere codes such as ATLAS [83,84] and TLUSTY [85]. ATLAS has, for example, been extensively used to model B stars. It can, for example, compute the atmospheric structure which can then be used in other codes to perform detailed non-LTE studies for individual atomic and ionic species (e.g., [86]). TLUSTY is fully non-LTE, and has also been used to interpret both B and O star spectra. However, even for photospheric lines, spherical codes that allow for the stellar wind have an advantage over plane-parallel codes. In particular, they allow for back warming caused by the wind [87] which will influence the temperature structure, they model the wind profiles, and there is no artificial distinction between the wind and photosphere as in SEI.

Examples of codes based on spherical geometry that have been used to model the UV of massive stars include WM-BASIC [88], POWR (e.g., [89,90]), METUJE [91] and CMFGEN [92,93]. FASTWIND (e.g., [94,95]) which has been used for extensive optical studies, has recently been updated to model the UV spectral region [96]. In order to facilitate the calculations, these codes compute the radiation field in the comoving-frame. The "observed" spectrum can be computed using either the comoving-frame calculation (as with WM-BASIC) or a secondary calculation in the observer's frame (as with CMFGEN). Excellent spectral fits can be achieved (Figure 3). Most of the calculations with CMFGEN and POWR use a prescribed mass loss and velocity while WM-BASIC and METUJE solve the radiation hydrodynamical equations. Recent advances to POWR allow the mass loss and velocity field to be computed for both O stars [97] and WR stars [98].

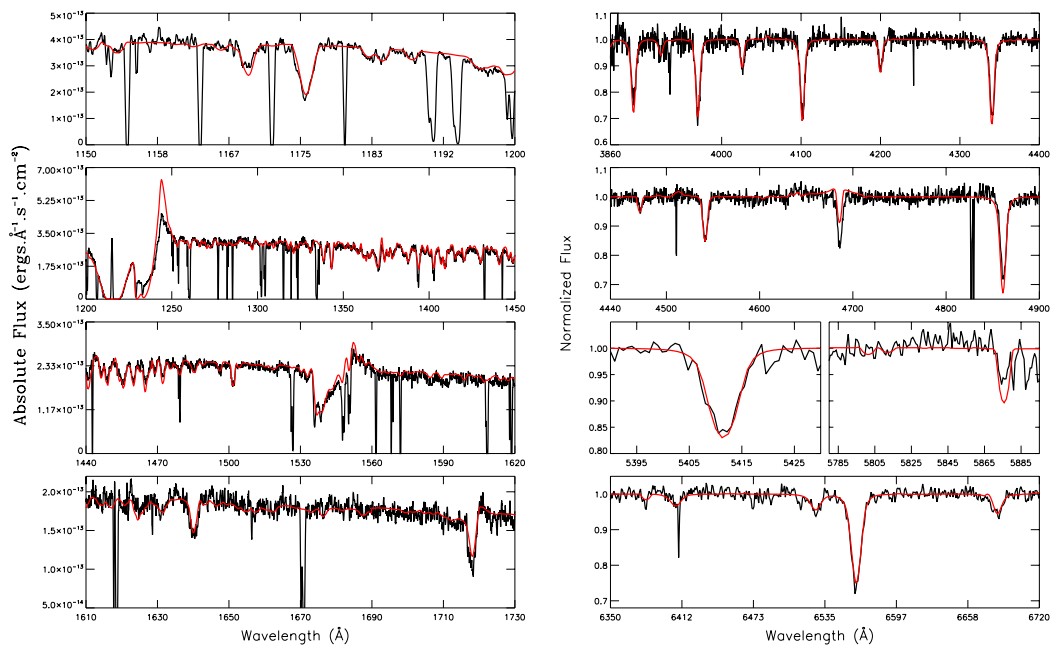


Figure 3. An illustration of a CMFGEN spectral fit to the SMC star AzV177 [O4V((ff))] [99]. The model has $T_{\text{eff}} = 44,500$ K, $\log g = 4.0$, $\log L/L_{\odot} = 5.43$, $\dot{M} = 1.4 \times 10^{-7} M_{\odot} \text{ yr}^{-1}$, $V_{\infty} = 2400 \text{ km s}^{-1}$, and $f = 0.05$ ($D = 20$). Credit: Bouret et al., A&A, 2013, 555, A1 [99], reproduced with permission © ESO.

Extensive UV calculations of O star spectra have been undertaken using WM-BASIC [100,101]. These pioneering calculations used an improved form of CAK wind theory [102] to compute the mass-loss rate and the velocity law from first principles, and allowed for extensive line blanketing [103].

4.2. Models with Rotation

Most O-star spectral modelling accounts for rotation by using a convolution technique (see, e.g., [104]). For photospheric absorption lines this technique gives line profiles that are in good agreement with profiles computed by performing a formal integration across the stellar disk. However, in some cases line profiles can have a very strong center-to-limb variation, and in such cases very different profiles are obtained. In ζ Puppis, for example, the double-peaked N IV $\lambda 4058$ emission line is a direct consequence of rotation [105].

In the wind, conservation of angular momentum indicates that the rotation rate will decrease as the material moves from the star, and if only radial forces acted, conservation of angular momentum would imply that the trajectory of a blob of wind material would lie in a plane centred on the star [106]. However simulations show that non-radial forces cannot be neglected [107].

Another complicating issue is that the effective temperature and surface gravity are not constant for a rotating star. These effects are very important for stars rotating near breakup, but are generally neglected for O stars. The effects can be complicated—at the equator the lower effective gravity will enhance the wind but this can be offset by the reduction in effective temperature (e.g., [108]). Further complications arise because of the influence of the Eddington limit, and because opacities are not a monotonic function of temperature (e.g., [109]).

4.3. Binaries

If the components of a binary are non-interacting, and if both spectra can be seen, they can be analysed using the same techniques as for single stars. By using observations at multiple phases, and since the features of the different stellar components will exhibit distinct radial velocity curves, it is feasible to extract spectra of the individual components [110].

In “close” binary systems effects such as reflection and tidal distortion need to be taken into account. Typically these can be treated by decomposing the stars into a patchwork layer, and then using 1D models to model each region (e.g., [111,112]). The spectra are then summed to produce a spectrum.

When one star has a wind it is possible to use the “secondary” star to probe the wind of the primary star. Such a technique was used, for example, to probe the size and effective temperature of the WR star in the OB+WR binary V444 Cygni [113,114]. It was also used to demonstrate the importance of Fe in the UV spectral region in WR stars [115,116].

In general, the analysis of stellar spectra for binary stars with stellar winds is much more complicated than for single stars, and detailed work on UV spectral modelling is limited. In such systems there is a bow shock formed by the collision of two winds, and this collision will generate X-rays. Depending on the density of the winds, the shocks may be isothermal (in which case large density enhancements will be produced that can give rise to line emission) or adiabatic (e.g., [117]). In addition, the radiation from one star can alter the wind of the other star [118,119]. In general, disentangling techniques do not work since the line profile shapes vary with orbital phase. This effect is clearly seen, for example, in the WR binaries WR 79 [120] and HD 5980 (e.g., [121,122]), and in Eta Carinae (e.g., [123]).

Monte Carlo methods have the potential to model complex binary systems with colliding winds. MC methods are routinely used to model, for example, SNe (e.g., [124–126]). Non-LTE MC codes have also been used to study disk winds in cataclysmic variables (CVs) (e.g., [127–129]) and Be stars (e.g., [130]). These codes tend to use the Sobolev approximation for the line transfer, which is reasonable for winds and SNe, but they cannot be used to study the photospheres and the acceleration of the wind around the sonic point. The interpretation of the complex line profiles seen in Eta Carinae (particularly those belonging to He I) will require detailed non-LTE modelling on a variety of spatial scales. To date, there has only been approximate non-LTE modelling of the ionisation structure of the colliding winds in Eta Carinae [131,132].

5. UV Nuggets

In this section we highlight a few key results (necessarily incomplete) facilitated by UV observations and their analysis.

5.1. Mass-Loss Diagnostics Using UV Spectral Lines

With the advent of FUSE, spectra from 900–1200 Å became available. A study of O supergiants in the Magellanic Clouds led to a revision in the stars’ temperatures, and a realisation that the winds of these stars are clumped [42]. In particular, the strength of P v $\lambda\lambda 1118, 1128$ could only be made consistent with wind parameters derived from other lines by invoking clumping. The models of two SMC stars (AzV 83 and AzV 69) by [133] also required the inclusion of clumping. Of particular interest was the O7 Iaf+ supergiant AzV 83 which has a moderately dense wind. Importantly, the UV spectrum contains both numerous wind diagnostics and a visible photospheric spectrum. Unclumped models developed to fit emission lines (such as H α) failed to fit P v $\lambda\lambda 1118, 1128$, and strong UV photospheric lines such as O IV $\lambda\lambda 1339, 1343$. Again, clumping needed to be invoked. Using a mass-loss rate derived from unclumped models, the UV lines were skewed to the blue (a consequence of motions at the base of the photosphere), and this was not observed. The advantage of using distorted photospheric lines to constrain the mass-loss rate is that they should not be sensitive to porosity.

One of the most important results came from FUSE observations which showed that the P v $\lambda\lambda 1118, 1128$ doublet in a large number of O stars was much weaker than expected, implying that the mass-loss rates of O stars were much lower than those derived from H α observations or that phosphorous was very underabundant [43,44]. Importantly, the P v $\lambda\lambda 1118, 1128$ doublet was unsaturated, and in many O stars, P⁴⁺ was expected to be the dominant ionisation stage which, in principle, allows a direct estimate of the mass-loss rate. Another result was obtained by comparing results from the analysis of doublets. Due to the different oscillator strengths, the red component of the

O VI, P V, N V, C IV, Si IV doublets have optical depths a factor of two lower than the blue component. However, analysis of UV wind profiles in B stars showed that the best fits to the doublet profiles were generally obtained using a ratio less than two, indicating that the winds are porous [134,135].

5.2. The Extreme Ultraviolet

In many massive stars much of the flux is emitted in the extreme ultraviolet (EUV) shortward of the Lyman limit at 911 Å. This region is also responsible for supplying much of the momentum used to drive the wind in many massive stars. Unfortunately in most massive stars this region is unobservable. However one nearby star, ϵ CMa (B2II), has had the EUV/soft X-ray spectrum observed [136,137]. Detailed studies of ϵ CMa showed that the EUV flux was at least an order of magnitude brighter than that predicted by ATLAS or TLUSTY model atmospheres [136,137]. Later work by [138] showed that the discrepancy can be reduced by making allowance for the transonic velocity field in the stellar wind. In ϵ CMa, the emission lines at shorter EUV wavelengths, and the X-ray flux ($E > 100$ eV), significantly affect the ionisation structure of the stellar wind [139].

The second way the EUV flux can be studied is through its influence on the ionisation balance in H II regions (e.g., [140]). With high quality data and sophisticated modelling, it is possible to place constraints on the photon flux emitted at wavelengths shortward of various ionisation edges – H I (13.6 eV), He I–II (24.6, 54.4 eV), O I–III (13.6, 35.1, 54.9 eV), C II–IV (24.4, 47.9, 64.5 eV), N I–III (14.4, 29.6, 47.4 eV), Ar I–III (15.8, 27.6, 40.7 eV), and Si I–IV (10.4, 23.3, 34.9, 47.2 eV) (see Figure 1 in [140]). In general there is broad agreement between the model UV fluxes and those needed to reproduce the observed emission lines (e.g., [141–145]). Ref. [140] suggest that it might be possible to reverse-engineer the line ratios to constrain the ionising radiation field. This would provide crucial insights into star-forming regions where multiple sources are contributing to the ionising radiation field.

5.3. Weak Winds

Analyses of UV resonance lines indicate that a subset of O stars have mass-loss rates that are much lower than expected theoretically. There are two classes (which overlap) of objects in this category. The first class, defined purely spectroscopically, are the Vz stars. These are main-sequence O stars that show much stronger He II $\lambda 4686$ absorption than normal OV stars (e.g., [146]), and appear to have weak winds for their spectral type. It was postulated that the He II $\lambda 4686$ absorption in normal class V stars is already contaminated by emission, and that Vz stars are lower luminous objects close to the zero-age main sequence (ZAMS). However work by [147] suggests that while age may be an important factor for the Vz class it is also possible to find examples of OV Vz stars that have similar properties to normal OV dwarfs. They note that in the LMC the Vz phenomenon may (partially) arise from lower density winds arising from the lower metallicity of the LMC.

The second class of “weak-wind” stars was identified by [148] and refers to stars that have mass-loss rates an order of magnitude lower than that predicted for their spectral type at the time. The two stars were main-sequence stars, and had luminosities less than $2 \times 10^5 L_{\odot}$. Similar stars, with very low mass-loss rates, were found in the study of MSC-N81 by [149] who suggested that the wind-luminosity relation for dwarfs breaks down when $L < 3 \times 10^5 L_{\odot}$. Similar “weak-wind” stars are found in the Galaxy [150,151] although the upper $L < 2 \times 10^5$ limit to the phenomenon may be a little lower than in the SMC. [151] suggest that evolution may not be a crucial parameter—they found that O9–O9.5III stars also exhibited weak winds. The “weak wind” problem is also seen for non-supergiant B stars [152]. There has been a suggestion that the weak wind problem is related to issues in driving the flow below the sonic point [153].

Mass-loss rates for the “weak-wind” stars have typically been determined from UV observations—the influence of the wind on lines in the optical spectrum can only provide an upper limit to the mass-loss rates (e.g., [154]). As discussed in Section 7.2, there are several issues that complicate the determination of UV mass-loss rates. One issue that may be important for these stars with the small mass-loss rates is that gas shocked by radiation-driven wind instabilities may not cool. Thus the

clumping properties of the wind will be distinct, and a large component of the wind may be hot and hence undetectable by UV observations.

5.4. Superions

With the availability of extensive UV observations it was discovered that the UV of O stars exhibited P Cygni profiles of species whose existence was incompatible with the effective temperature of the star [34]. In the earliest O stars, lines due to N V $\lambda\lambda$ 1238, 1242 and O VI $\lambda\lambda$ 1031, 1038 fall into the superion category while in later spectral types C IV $\lambda\lambda$ 1548, 1552 also falls into this category.

Ref. [34] suggested that this indicated a warm corona of 10^5 K existed around the stars, however such a corona would be very difficult to maintain because of strong cooling at this temperature. The now commonly accepted explanation, as first suggested by [155], is that these high-ionisation lines are produced via Auger ionisation—that is, high energy X-rays eject an inner shell electron (a 1s electron for CNO). The highly excited ion then ejects a second (or more for species of a high atomic number) electron as it reconfigures itself. Thus, for example, $O^{3+} + X\text{-ray} \rightarrow O^{5+} + 2e^-$. The success of EUV, and X-rays arising from shocks, in explaining the presence of superions has been confirmed by many detailed spectral calculations (e.g., [88,100,156,157]). Most spectral calculations now take the EUV and X-rays into account when performing UV spectral synthesis calculations.

For some time the origin of the X-ray emission was unclear. The X-rays could arise in a hot corona at the base of an otherwise cool wind [155,158], or they could arise from shocks distributed in the wind. With the advent of X-ray observations, the detection of soft X-rays (e.g., [75,159]), and the analysis of X-ray line profiles (e.g., [160]), it is now commonly accepted that in single O stars the X-rays arise from shocks distributed throughout the wind. In binaries, colliding winds give rise to a strong X-ray flux (e.g., [76,161,162]).

Initial modelling of the UV superions assumed the winds were smooth and homogeneous. However it is now generally accepted that the winds are clumped, and this can have a profound influence on the formation of the superion profiles. [157] showed, for example, that the strength of lines due to the superions is strongly influenced by the interclump medium. Indeed, the interclump medium may be more important for producing the lines than are the clumps—this is simply a consequence of the higher ionisation in the interclump medium which occurs because of its lower density. The interclump medium may also be crucial for the observed “blackness” of P Cygni profiles (e.g., [81]).

5.5. Non Galactic/Magellanic Studies

A major thrust for detailed modelling of UV spectra is to understand the origin of the elements and the nature of the first stars. The first generation of stars (Pop III) will have zero metallicity, and thus their wind properties will be very different from stars within the local group. The SMC, itself, does illustrate the importance of metallicity on stellar properties, and their winds, but stars in the SMC are still relatively “metal-rich”—their metallicity is only a factor of five lower than our Galaxy. Potentially, “nearby” dwarf galaxies offer a means to probe winds at lower metallicities. Two such galaxies are IC 1613 and the dwarf irregular galaxy, Wolf-Lundmark-Melotte (WLM). Pioneering observations suggested that the mass-loss rates were higher than expected for a low metallicity galaxy [163]. However, an analysis of three O stars showed that both galaxies actually have metallicities similar to the SMC [164]. Such a metallicity is similar to that inferred by [165]. One potential caveat is that the measured Fe/H ratio is sensitive to the adopted microturbulence. Moreover, while the derived mass-loss rates were higher than those predicted by [166], they were in agreement with the predictions of [167]. There is an urgent need for a new large UV telescope (Diameter: 6 to 10 m) to facilitate the study of massive stars in more distant, and very low metallicity galaxies, such as I Zwicky 18 (e.g., [168]). See, for example, the discussion by [169].

While the advent of a new large UV telescope to access low-metallicity galaxies, etc. is essential, the Ultraviolet Legacy Library of Young Stars as Essential Standards (ULLYSES) will provide crucial data that will allow current and future generations to address some of the fundamental questions

related to massive stars and starbursts. The ULLYSES data will provide insights into stellar winds, insights into the influence of rotation and binarity on stellar evolution, and fundamental data, such as spectral templates, for the interpretation of star formation and starbursts in external galaxies. In addition, the data will help facilitate advancements in the model atmosphere codes that are crucial for interpreting spectral data, for supplying theoretical spectra for wavelength regions not directly observable, and for supplying spectral templates of stars that cannot be directly observed.

5.6. The Iron Forest

In O and B stars iron transitions dominate the UV photospheric spectrum, and iron is one of the most important line-blanketing species. This is due to the combination of its abundance and its atomic structure. The important Fe ions in O and B stars have incomplete 3d and 4s sub-shells. The lowest states are all of even parity, and there are many such states due to the many possible $3d^n 4s^m$ terms. Excitation of one of the valence electrons to the 4p shell gives rise to the first set of odd terms.

As a consequence of the term structure and ionisation, different iron ionisation stages dominate different regions of the UV spectrum (Figure 4). One difficulty in analysing the UV is that accurate transition wavelengths for many species are unknown. The situation has improved for Fe II but is much worse for higher ionisation stages of iron, and for other iron group elements.

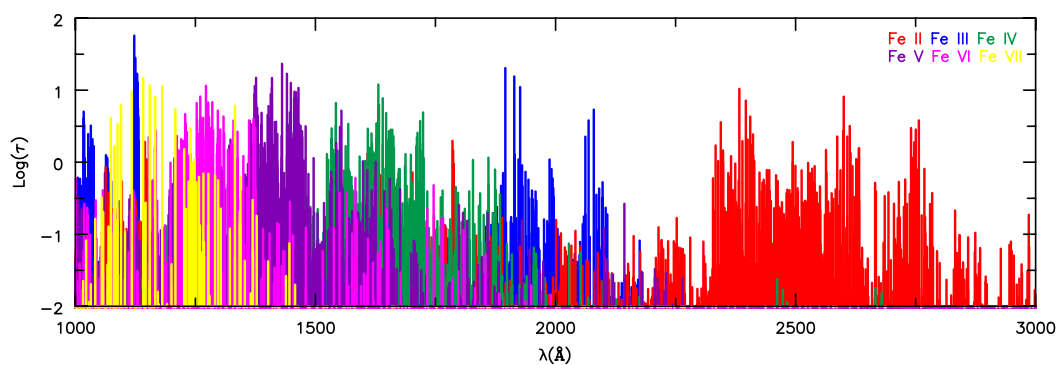


Figure 4. Illustration of the location of the strongest Fe lines in the UV spectral window. Different ionisation stages tend to dominate different spectral regions.

An accurate determination of the Fe abundance is important because at most metallicities it plays a significant role in determining the mass-loss rate (e.g., [98,170–173]). Moreover, it is responsible for the Z-opacity bump [174]. The Z-bump is the name given to the enhancement in the Rosseland mean opacity at temperatures of around 200,000 K that arises from iron, and other iron group elements. In massive stars, radiation pressure makes a significant contribution to the total pressure—indeed many stars are close to the classical Eddington limit. The “classical” Eddington limit is computed by assuming that H and He are fully ionised, and that electron scattering is the only opacity source. The Z-bump enhances the opacity (via bound-free and bound-bound processes) and lowers the effective Eddington luminosity. This can result in density inversions, the creation of a weak convection zone, and inflated atmospheres (e.g., [175–177]). The latter two may be important for understanding the density structure of the sub-photospheric layers in WR stars. Convection may also be important for understanding the origin of microturbulence in O and WR stars (e.g., [53,178]), and perhaps for the initiation of instabilities in radiation-driven winds.

6. Other Classes of Massive Stars

6.1. Modelling of Wolf–Rayet Stars

Extensive modelling of WR stars in our Galaxy (e.g., [19,179,180]) and in the Magellanic Clouds (e.g., [181–184]), and more limited modelling of WR stars in other galaxies (e.g., [185]), has been

undertaken primarily using CMFGEN and POWR. Most recent modelling utilises both optical and UV observations (when available). In general the agreement between tailored models and observations is reasonable. Discrepancies do exist, although it is difficult to discern the cause of these discrepancies. Some lines are very model-sensitive (e.g., C III λ 5696 in WC stars [92]) and it is not surprising that spherical and semi-homogeneous (i.e., smooth but using a clumping factor) models struggle to match the line. Some of the discrepancies are undoubtedly due to inaccuracies in the adopted atomic models. Fortunately, there are many features in Wolf–Rayet spectra which allow strong constraints on the luminosity, the mass-loss rate, and abundances to be derived.

The influence of clumping in WR stars is easily discerned by the relative weakness of redshifted electron scattering wings on emission lines³, since (recombination) line emission typically scales as the density squared while the electron scattering optical depth only scales as the density (e.g., [188]). While $f = 1$ is clearly incompatible with the observations, it is difficult to provide an accurate determination of f . In WNE and WCE stars values of f less than 0.2 are fairly consistent with observations, and values of $f = 0.1$ ($D = 10$) and $f = 0.05$ ($D = 20$) are routinely used in the literature (e.g., [55,179,180]). Several factors contribute to the difficulty of deriving more accurate f values including possible systematic uncertainties in the models, blending (particularly in the UV and in WCE stars), and the need for very accurate continuum definition (since the electron scattering wings tend to be broad, weak, and only seen on the red side). Unfortunately, derived mass-loss rates are necessarily uncertain since it is \dot{M}/\sqrt{f} that is mostly derived from fitting of the spectra. In some P Cygni stars (such as P Cygni itself) the electron-scattering wings are easily discernible [186], appear on both sides of the line profile (since V_∞ is less than the mean electron thermal speed), and hence can be used to place firm constraints on f (e.g., [189,190]).

Iron is a very important opacity source in WR stars, particularly shortward of 1500 Å [113–115,191] (Figure 2). In principle the iron abundance could be derived from these emission lines but because of reddening, and the severe blending, modellers routinely adopt the iron abundance determined from “young” stars within the same galaxy.

In order to improve our knowledge of WR stars in the Magellanic Clouds [184,192] undertook a survey looking for new WR stars. They found 10 unusual WR stars which were classified as WN3/O2 and had absolute visual magnitudes fainter than -3.1 —too faint to be a WN3 and an O3 binary. Their effective temperatures are of order 100,000 K, their H/He ratios are of order unity (by number), and (for Wolf–Rayet stars) they have very low mass-loss rates— $\sim 10^{-6} M_\odot \text{ yr}^{-1}$ [184]. Unusually, in the three stars with UV data, C IV $\lambda\lambda$ 1548, 1552 is not seen—indicative of their high effective temperatures, low mass-loss rates and abundances of CNO that are consistent with full CNO processing. The strongest UV lines are O VI $\lambda\lambda$ 1031, 1038, N V $\lambda\lambda$ 1238, 1242, and He II λ 1640, and unlike for most WR spectra, the UV continuum can be readily identified [192]. As extensively discussed by [192] the nature of these stars is uncertain. As they are not fast rotators they probably do not arise via quasi-homogeneous evolution or from a merger. Current single star models cannot explain their position in the HR diagram, although older (less physical) models could. In one sense these stars are more similar to what was originally expected for a WR star—an object that is very hot and compact. [193] take an alternative point of view, and argue that the stars arise from non-conservative mass-transfer onto a low mass companion.

³ In the optical and UV we can assume that the scattering of a photon by an electron is coherent in the frame of the electron (we can ignore the Compton shift). However, in the observer’s frame the scattered (line) photon will be either blueshifted or redshifted depending on relative motion of the electron relative to the source and the observer. In stars like P Cygni, the random thermal motions of the electrons are larger than the wind speed, and profiles typically show symmetric wings with a characteristic width of order 1000 km s^{-1} (e.g., [186]). However, in WR stars the outflow velocities are larger than typical thermal speeds, and we preferentially see an electron scattering wing on the red side of the line profile [187]. Recall that in an expanding flow with a monotonic velocity, the source is always receding from the scatterer.

6.2. O Stars with Strong Magnetic Fields

About 6% to 7% of O stars are found to have strong ($B > 100$ Gauss) magnetic fields, and several have very extreme fields [194,195]. NGC 1624-2 (Of?p), for example, is a main-sequence star with an effective temperature of 35,000 K, $\log g = 4.0$, a longitudinal magnetic field of around 5 kG, and a surface dipole magnetic field greater than 20 kG [196]. The star shows very significant variations in wind lines between its high and low states [197]. The authors use the Analytic Dynamical Magnetosphere (ADM) formalism of [198] to interpret the variations. In these O stars with strong magnetic fields, the magnetic field is strong enough to channel the wind toward the magnetic equator creating shocks and dynamically complex gas flows.

Another example of a magnetic star is HD 108 which has a 1–2 kG field [199]. Spectral variations are seen in both optical and UV wind lines on a timescale of decades, and are most likely related to the rotation period of the star [199,200], and the misalignment between the magnetic and rotation axes [199] although intrinsic wind variations cannot be ruled out [200].

A misalignment between the magnetic and rotation axes can also explain the observed variability in HD 191612 (Of?p) [201]. HD 191612 also shows strong variability in $H\alpha$ with a period of 584 d [202] and is estimated to have a dipole field with $B = 2450 \pm 400$ G [203].

6.3. LBVs

Since LBVs are transition objects they are potential goldmines for advancing our understanding of stellar evolution. As their name implies, LBVs are not a well-defined class—they are simply luminous, blue and variable. There are irregular small amplitude fluctuations in brightness, there are the S-Dor variations in which the visible magnitude can change by over one magnitude but which occur at roughly constant luminosity (but see [190]), and there are the large outbursts in which many solar masses of material can be ejected (e.g., [204]). As a class they are poorly understood. This arises because of their short lifetime, and because multiple evolutionary channels can be contributing to members of the class, leading to confusion. Below we discuss three of the most famous LBVs.

P Cygni is a B supergiant. Assuming a distance of 1.7 kpc it has the following parameters: $R_* = 76 R_\odot$, $T_{\text{eff}} = 18,700$ K, $L \sim 6 \times 10^5 L_\odot$, $V_\infty = 185 \text{ km s}^{-1}$, and $\dot{M}/\sqrt{f} = 3.3 \times 10^{-5} M_\odot \text{ yr}^{-1}$ [189,205]. Using the electron scattering wings on the Balmer lines, a rather high clumping value ($f = 0.5$ ($D = 2$)) is derived. This large value is probably due to the much lower terminal velocity of the stellar wind, and hence the lower amplitude of the shocks that are created by radiation-driven instabilities. Excellent fits to both the optical and UV spectra are obtained, and are illustrated in [189]. Given the advances in atomic data, and our understanding of stellar winds, and the importance of the observable UV for the stellar wind, it would be very worthwhile to revisit models for this star.

Another well-studied LBV is AG Car. Detailed spectroscopic modelling has shown that the star is a fast rotator, and during outburst (when the star become visually brighter but fainter in the UV) it has a lower luminosity ($1 \times 10^6 L_\odot$) than during minimum ($1.5 \times 10^6 L_\odot$) [190]. Excellent fits to the UV and optical spectra were obtained [190]. A comparison of a CMFGEN model with observations is shown in Figure 5.

The final LBV to be discussed is HD 5980 in the SMC. This is a binary system containing (at most epochs) two WN stars with a period of 19.3 d. It may actually be a quadruple system—spectra are contaminated by light from a third star which is also a binary (e.g., [206]). During 1994 it underwent an LBV-like outburst, which was very unusual since its effective temperature during minimum is much higher than for other LBVs. The two WN stars are estimated to have masses of $\sim 60 M_\odot$ [206], and effective temperatures of around 50,000 K [122,207,208]. UV monitoring shows complex variability of the main resonance profiles as a function of orbital phase and in time [122]. These variations are not well understood but will provide insights into the wind structures of the two stars. HD 5980 highlights the LBV enigma. Is binary interaction responsible for the LBV phenomenon or can it occur in single stars? If binary interaction is not crucial, do all stars in some mass range undergo LBV variations that

where f_{lu} is the oscillator strength, n_l is the number density of the lower level, m_e is the electron mass, c is the speed of light, λ is the transition wavelength, and we have neglected stimulated emission⁴. Using $\zeta_i = n_l/N$ (N total atom/ion density of all species),

$$\dot{M} = 4\pi r^2 \rho V_\infty, \quad (2)$$

$$\rho = \mu m_{\text{amu}} N, \quad (3)$$

with \dot{M} the mass-loss rate, ρ the density, and m_{amu} the atomic mass unit, and assuming the classic β -velocity law,

$$v(r) = V_\infty (1 - R_*/r)^\beta, \quad (4)$$

the optical depth at large radii is given by

$$\tau = 2.3 \times 10^3 \left(\frac{f_{lu}}{0.2} \right) \left(\frac{\lambda}{1000 \text{ \AA}} \right) \left(\frac{\zeta_l}{10^{-4}} \right) \left(\frac{1000 \text{ km s}^{-1}}{v} \right)^2 \left(\frac{\dot{M}}{10^{-6} M_\odot \text{ yr}^{-1}} \right) \left(\frac{1}{\beta\mu} \right) \left(\frac{10R_\odot}{R_*} \right). \quad (5)$$

As readily apparent from this expression, the optical depth for strong resonance lines of CNO elements will typically exceed unity when the flow has reached terminal speed. Thus we would expect the UV edge of resonance transitions to exhibit an almost vertical edge rising from zero to the continuum. In reality this is not observed—the UV edge is typically sloped over several hundred km s^{-1} (see Figure 6). It is now generally accepted that this high-velocity, non-black absorption is associated with high velocity and low density gas that arises from the shock produced by radiation-line-driving instabilities. As a consequence, [211,212] proposed that a better measure of V_∞ is V_{black} which is the maximum velocity associated with the saturated black portion of the P Cygni profile.

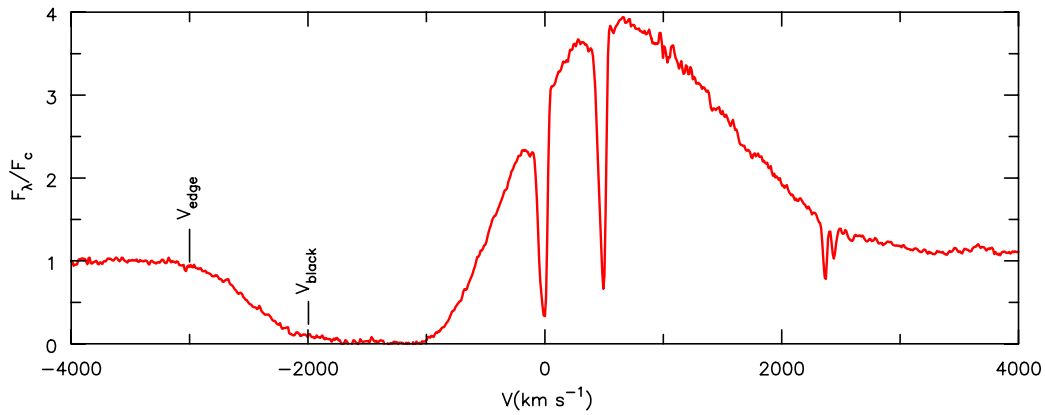


Figure 6. Illustration of the C IV $\lambda\lambda 1548, 1552$ P Cygni profile in HD 50896 (WN5). V_{edge} and V_{black} are marked. Due to observational errors, both V_{edge} and V_{black} are generally difficult to measure accurately. In the present case, the weak emission in the P Cygni trough means that V_{edge} is close to 3000 km s^{-1} while V_{black} lies between 1700 and 2250 km s^{-1} . The value of 1700 km s^{-1} is inferred when we use the deepest blue extent, while the higher value refers to the clear change of slope that occurs in the bottom of the P Cygni profile. As is generally observed, the emission peaks close to the intrinsic location of the redward doublet component (as indicated by the strong C IV interstellar absorption feature). IUE data is from [213], and was kindly supplied to the author by Ian Howarth.

For WR stars, particularly the strong-lined WR stars, terminal velocities can be gleaned from optical transitions—He I lines in WNE stars, and He I and C III lines in WCE and WO stars. In these

⁴ The expression for the radial optical depth is only valid when the Sobolev length ($V_{\text{Dop}} \cdot dr / dv$) is less than the wind scale length (r).

stars the isolated He I lines typically show a flat-topped profile with weak P Cygni absorption, while many of the C III lines are trapezoidal (flat-topped) but lack P Cygni absorption. For HD 50896, V_{edge} is close to 3000 km s^{-1} while V_{black} lies between 700 and 2250 km s^{-1} . As part of his thesis, Hillier used the He I and the general spectrum fit, to deduce a low terminal velocity of around 1700 km s^{-1} for HD 50896, much less than the value inferred from the blue edge of the C IV $\lambda\lambda 1548, 1552$ transition [214]. A value of close to 2000 km s^{-1} is probably to be preferred. It has been shown by [80,188,215] that the microturbulence that is assumed for the intrinsic line profile in spectral modelling leads to a redshift of the emission line. However, the microturbulence used to characterise this shift is related to the dense clumps, and may have little direct relation to the turbulence of the low density material generating the absorption extending shortward of V_{black} .

In WCE stars the C IV $\lambda\lambda 1548, 1552$ resonance doublet exhibits a very large redshift ($\sim 1000 \text{ km s}^{-1}$). This shift arises from radiative transfer effects and is due to the very high optical depth of the resonance transition [92] and the need to use a Lorentzian line profile. When this is done, there is much better agreement between the observed and model C IV resonance profiles (Figure 7).

Constraints on the velocity law can also be obtained using UV resonance lines. Typically it is found that most profiles (including optical lines such as $H\alpha$) can be fit using a classic $\beta = 1$ velocity law although there are cases where higher values ($\beta = 1.5$ to 3) are required to explain the observations. The use of a single parameter, such as β , to describe the velocity law introduces confusion, since β determines both the acceleration of the wind close to the star, and the asymptotic acceleration to the terminal speed. There is no reason, a priori, that these should be governed by the same parameter. For O stars, large β values are somewhat problematical since they indicate that gravity is almost exactly balanced by radiation pressure in the wind. As for mass-loss rates, clumping, porosity, and departures from spherical geometry will introduce systematic errors into the determination of the velocity law. Ideally we could determine the velocity law from hydrodynamic simulations, and such simulations do tend to lead to a $\beta \approx 1$ velocity law (Equation (4)). Since clumping and porosity will influence the radiative force, the velocity law needs to be determined in conjunction with the inhomogeneous density structure. In 3D this is a challenging problem. Clumping can also influence the optically thick region, since clumping can hide “opacity”, and hence lower the radiative force [216]. This can allow steady-state super-Eddington winds (e.g., [217,218]).

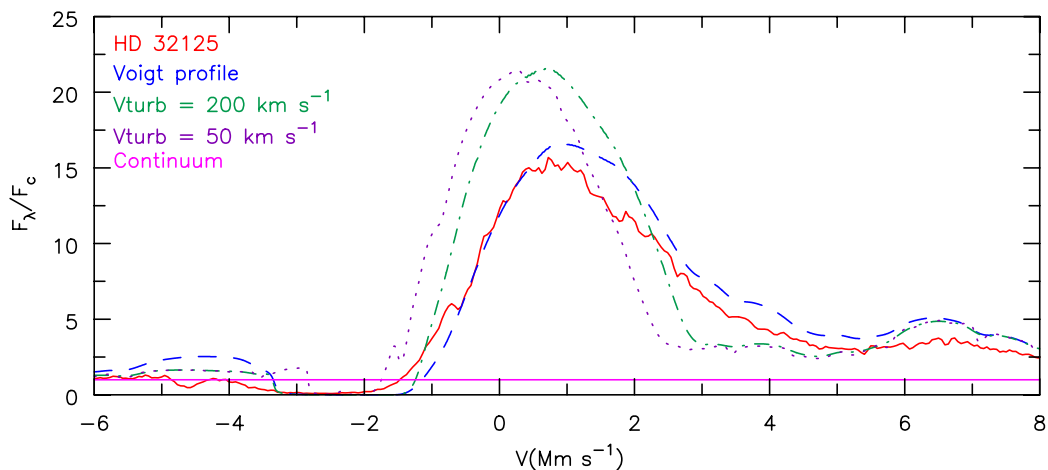


Figure 7. Illustration of the influence of an adopted intrinsic line profile in the formal solution on the C IV $\lambda\lambda 1548, 1552$ profile. Three theoretical profiles are shown: A Voigt profile with $V_{\text{turb}}(\text{max}) = 200 \text{ km s}^{-1}$ (dashed, blue), a Doppler profile with $V_{\text{turb}}(\text{max}) = 200 \text{ km s}^{-1}$ (dot-dashed, green), and a Doppler profile with $V_{\text{turb}}(\text{max}) = 50 \text{ km s}^{-1}$ (dotted, purple). These are compared to the observed profile of the LMC WC4 star HD 32125 (red). Zero velocity refers to the wavelength of the red component at 1550.18 \AA . Unlike for the vast majority of emission lines, the choice of the intrinsic line profile has a very significant effect on both the shape and centroid of the C IV $\lambda\lambda 1548, 1552$ emission profile.

7.2. On the Accuracy of UV Mass-Loss Rates

A major requirement for advancing our understanding of stellar evolution is the need for accurate mass-loss rates. Unfortunately mass-loss rates derived from UV observations can be influenced by multiple systematic errors. The source of these systematic errors is directly attributable to the unstable nature of line-driven winds. It is convenient to separate these into four classes— X-rays, clumping, spatial porosity and vorosity. This distinction is physically artificial—these are most likely all related to the inherent instability of radiation-driven stellar winds.

X-rays were also discussed in Section 5.4. In stars with strong winds (BSGs and WR stars) many wind lines are insensitive to X-rays, and the treatment of X-rays does not appear to have a large influence on derived mass-loss rates. For “weak-wind” stars, very high X-ray filling factors are needed (essentially the whole wind must be hot) to explain the observed X-ray emission. As a consequence the wind dynamics, X-ray formation, and UV lines formation should be treated simultaneously.

The influence of porosity can be studied by looking at UV doublets, since for prominent UV resonance lines the optical depths differ by a factor of two. An ideal line in cooler O (and B) stars is Si IV $\lambda\lambda$ 1394, 1403 due to its wide separation. When porosity is important, unsaturated doublet profiles cannot be simultaneously fit with the same atmospheric structure (e.g., [134]). A simple example of the phenomena is shown in Figure 8.

To compute mass-loss rates, accurate distances are needed, and these have generally only been available for stars in the Magellanic Clouds. However, with the releases of data from GAIA, improved distances are becoming available for galactic stars, leading to improved mass-loss rates and stellar parameters (e.g., [17,219,220]). To a very good approximation, mass-loss rates derived from old distance estimates can simply be scaled— $\dot{M}_{\text{new}} = \dot{M}_{\text{old}} \times (d_{\text{new}}/d_{\text{old}})^{1.5}$.

Assuming an accurate distance estimate, it is probably fair to assume that derived mass-loss rates are accurate to better than a factor of two. Mass-loss rates based on H α emission (in O Stars) and other emission lines (in WR stars and LBVs) that assume a smooth wind (i.e., $f = 1$) appear to provide a reasonable upper limit. Mass-loss rates that use UV lines in conjunction with, for example, H α emission to determine both the mass-loss rate and the volume filling factor probably underestimate the mass-loss rates because of the neglect of porosity/vorosity.

For stellar evolution calculations, mass-loss prescriptions are required. Multiple prescriptions are available in the literature (e.g., [166,221–223]), and many of these are implemented in stellar evolution codes such as “Modules for Experiments in Stellar Astrophysics” (MESA) [224]. We will not attempt to decide on the merit and accuracies of various prescriptions—this would require a very lengthy review. Suffice to say that mass-loss rates across the HR diagram have significant uncertainties, and they should not be used blindly—changes in mass-loss rates of only a factor of two can have significant implications on stellar evolution (e.g., [225]). At present we do not understand why some stars have much lower mass-loss rates than expected (see Section 5.3), and there are also uncertainties related to the loss of angular momentum via stellar winds. Importantly, we still do not have a firm understanding of episodic mass loss (such as during an LBV phase), and such mass loss may be the most important for determining the subsequent evolution of the star (e.g., [226]). Finally we note that evolution of many massive stars is influenced by binary interaction and mass transfer.

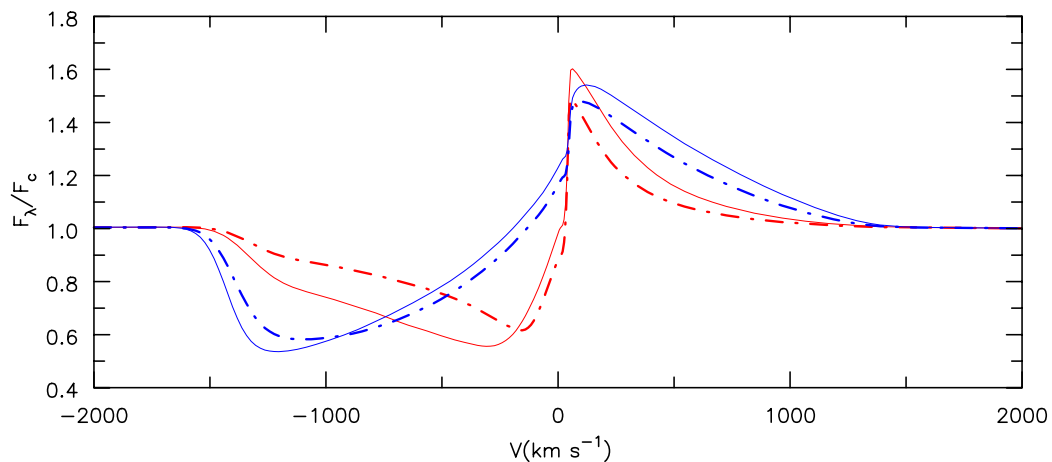


Figure 8. Illustration of the influence of porosity on non-overlapping doublets. In red we see example profiles for a non-porous wind. The dashed line has an oscillator strength a factor of two lower than the solid line, as is appropriate for the C IV, N V, and Si IV resonance doublets. As is readily apparent, the strength of the blueshifted absorption correlates well with the oscillator strength, and hence optical depth. For the blue profiles the optical depth was increased by a factor of 16 over the red profiles, however we assume that 50% of the continuum photons escape as a consequence of porosity. As a consequence the two lines have similar shapes, appear “unsaturated”, and the strength of the absorption correlates poorly with the optical depth. In reality the lines are “saturated”—both lines would have a residual minimum intensity close to zero if it were not for the effect of porosity. When the lines overlap the effects of porosity are more complicated (because the “bluer” line influences the profile of the “redder” line), however an analysis of the profiles can still provide information on the porosity of the wind.

8. Conclusions

The UV spectral region has revolutionised our understanding of massive stars and their stellar winds. Despite considerable advances, many questions about massive stars and their winds remain. These include the following: What is the relative importance of single and binary star evolution for determining the location of stars in the HR diagram, and their final evolutionary fate? What is the origin and nature of microturbulence and macroturbulence in O star photospheres? What is the detailed structure of massive star winds, and how do the properties depend on metallicity, and the rate of mass loss? What is the origin of the inconsistency between the evolutionary mass and the spectroscopic mass for some O stars? What is the cause of the discrepancy between the spectroscopic radii and evolutionary radii for some WR stars? What is the upper mass limit for a star, and how does this depend on metallicity? What mass ranges give rise to each class of SN, and do some massive stars simply collapse to form a black hole? What is the origin of magnetic fields that exist in a small fraction of O stars?

Funding: This review paper was not supported directly by any external funding. However the author is grateful for NASA support through multiple STScI grants (e.g., HST-GO-14476.002-A, HST-AR-14568.001-A, HST-GO-14683.002-A) and for direct NASA support (e.g., NASA Astrophysical Theory Program NNX14AB41G, NASA Astrophysics Data Analysis Program 80NSSC18K0729) that has allowed him to pursue studies of massive stars, radiative transfer and supernovae, and that did support some of the research reviewed in this paper.

Acknowledgments: The author thanks J.-C. Bouret, F. Najarro, J. Vink, and two anonymous referees for providing comments on an earlier version of this manuscript.

Conflicts of Interest: The author declares no conflict of interest.

Abbreviations

The following abbreviations are used in this manuscript:

CAK	Castor, Abbott, and Klein
CV	cataclysmic variable
DACs	discrete absorption components
BSG	blue supergiant
FUSE	Far Ultraviolet Spectroscopic Explorer
HR	Hertzsprung-Russell
IUE	International Ultraviolet Explorer
LBV	luminous blue variable
LMC	Large Magellanic Cloud
MC	Monte Carlo
RSG	red supergiant
SMC	Small Magellanic Cloud
SN(e)	supernova(e)
ULLYSES	Ultraviolet Legacy Library of Young Stars as Essential Standards
YSG	yellow supergiant
WR	Wolf-Rayet
ZAMS	zero-age main sequence

References

1. Morton, D.C.; Spitzer, Lyman, J. Line Spectra of Delta and pi Scorpii in the Far-Ultraviolet. *Astrophys. J.* **1966**, *144*, 1. [[CrossRef](#)]
2. Morton, D.C. The Far-Ultraviolet Spectra of Six Stars in Orion. *Astrophys. J.* **1967**, *147*, 1017. [[CrossRef](#)]
3. Beals, C.S. The Spectra of the P Cygni Stars. *Publ. Dom. Astrophys. Obs. Vic.* **1953**, *9*, 1. [[CrossRef](#)]
4. Groh, J.H.; Meynet, G.; Georgy, C.; Ekström, S. Fundamental properties of core-collapse supernova and GRB progenitors: Predicting the look of massive stars before death. *Astron. Astrophys.* **2013**, *558*, A131. [[CrossRef](#)]
5. Smartt, S.J. Progenitors of Core-Collapse Supernovae. *Annu. Rev. Astron. Astrophys.* **2009**, *47*, 63–106. [[CrossRef](#)]
6. Smartt, S.J. Observational Constraints on the Progenitors of Core-Collapse Supernovae: The Case for Missing High-Mass Stars. *Publ. Astron. Soc. Australia* **2015**, *32*, e016. [[CrossRef](#)]
7. Davies, B.; Beasor, E.R. 'On the red supergiant problem': A rebuttal, and a consensus on the upper mass cut-off for II-P progenitors. *Mon. Not. R. Astron. Soc.* **2020**, *496*, L142–L146. [[CrossRef](#)]
8. Farrell, E.J.; Groh, J.H.; Meynet, G.; Eldridge, J.J. The uncertain masses of progenitors of core-collapse supernovae and direct-collapse black holes. *Mon. Not. R. Astron. Soc.* **2020**, *494*, L53–L58. [[CrossRef](#)]
9. Dessart, L.; Hillier, D.J. The difficulty of inferring progenitor masses from type-II-Plateau supernova light curves. *Astron. Astrophys.* **2019**, *625*, A9. [[CrossRef](#)]
10. O'Connor, E.; Ott, C.D. Black Hole Formation in Failing Core-Collapse Supernovae. *Astrophys. J.* **2011**, *730*, 70. [[CrossRef](#)]
11. Sukhbold, T.; Woosley, S.E. The Compactness of Presupernova Stellar Cores. *Astrophys. J.* **2014**, *783*, 10. [[CrossRef](#)]
12. Meynet, G.; Chomienne, V.; Ekström, S.; Georgy, C.; Granada, A.; Groh, J.; Maeder, A.; Eggenberger, P.; Levesque, E.; Massey, P. Impact of mass-loss on the evolution and pre-supernova properties of red supergiants. *Astron. Astrophys.* **2015**, *575*, A60. [[CrossRef](#)]
13. Smith, L.F. A revised spectral classification system and a new catalogue for galactic Wolf-Rayet stars. *Mon. Not. R. Astron. Soc.* **1968**, *138*, 109. [[CrossRef](#)]
14. Torres, A.V.; Conti, P.S.; Massey, P. Spectroscopic studies of Wolf-Rayet stars. III—The WC subclass. *Astrophys. J.* **1986**, *300*, 379–395. [[CrossRef](#)]
15. Conti, P.S.; Leep, M.E.; Perry, D.N. The spectra of Wolf-Rayet stars. I. Optical line strengths and the hydrogen-to-helium ratios in WN type stars. *Astrophys. J.* **1983**, *268*, 228–245. [[CrossRef](#)]
16. Massey, P.; Hunter, D.A. Star Formation in R136: A Cluster of O3 Stars Revealed by Hubble Space Telescope Spectroscopy. *Astrophys. J.* **1998**, *493*, 180–194. [[CrossRef](#)]
17. Hamann, W.R.; Gräfener, G.; Liermann, A.; Hainich, R.; Sander, A.A.C.; Shenar, T.; Ramachandran, V.; Todt, H.; Oskinova, L.M. The Galactic WN stars revisited. Impact of Gaia distances on fundamental stellar parameters. *Astron. Astrophys.* **2019**, *625*, A57. [[CrossRef](#)]

18. Crowther, P.A.; Hillier, D.J.; Smith, L.J. Fundamental parameters of Wolf–Rayet stars. II. Tailored analyses of Galactic WNL stars. *Astron. Astrophys.* **1995**, *293*, 403–426.
19. Hamann, W.R.; Gräfener, G.; Liermann, A. The Galactic WN stars. Spectral analyses with line-blanketed model atmospheres versus stellar evolution models with and without rotation. *Astron. Astrophys.* **2006**, *457*, 1015–1031. [[CrossRef](#)]
20. Chan, C.; Müller, B.; Heger, A.; Pakmor, R.; Springel, V. Black Hole Formation and Fallback during the Supernova Explosion of a 40 M_{\odot} Star. *Astrophys. J. Lett.* **2018**, *852*, L19. [[CrossRef](#)]
21. Ensmann, L.M.; Woosley, S.E. Explosions in Wolf–Rayet stars and Type Ib supernovae. I—Light curves. *Astrophys. J.* **1988**, *333*, 754–776. [[CrossRef](#)]
22. Dessart, L.; Hillier, D.J.; Li, C.; Woosley, S. On the nature of supernovae Ib and Ic. *Mon. Not. R. Astron. Soc.* **2012**, *424*, 2139–2159. [[CrossRef](#)]
23. Taddia, F.; Stritzinger, M.D.; Bersten, M.; Baron, E.; Burns, C.; Contreras, C.; Holmbo, S.; Hsiao, E.Y.; Morrell, N.; Phillips, M.M.; et al. The Carnegie Supernova Project I. Analysis of stripped-envelope supernova light curves. *Astron. Astrophys.* **2018**, *609*, A136. [[CrossRef](#)]
24. Podsiadlowski, P.; Joss, P.C.; Hsu, J.J.L. Presupernova evolution in massive interacting binaries. *Astrophys. J.* **1992**, *391*, 246–264. [[CrossRef](#)]
25. Filippenko, A.V. Optical Spectra of Supernovae. *Annu. Rev. Astron. Astrophys.* **1997**, *35*, 309–355. [[CrossRef](#)]
26. Kuncarayakti, H.; Anderson, J.P.; Galbany, L.; Maeda, K.; Hamuy, M.; Aldering, G.; Arimoto, N.; Doi, M.; Morokuma, T.; Usuda, T. Constraints on core-collapse supernova progenitors from explosion site integral field spectroscopy. *Astron. Astrophys.* **2018**, *613*, A35. [[CrossRef](#)]
27. Woosley, S.E.; Heger, A. The Progenitor Stars of Gamma-Ray Bursts. *Astrophys. J.* **2006**, *637*, 914–921. [[CrossRef](#)]
28. Najarro, F.; Herrero, A.; Verdugo, E. Massive stars in the UV. *Astrophys. Space Sci.* **2006**, *303*, 153–170. [[CrossRef](#)]
29. Martins, F. UV, optical and near-IR diagnostics of massive stars. *Bull. De La Soc. R. Des Sci. De Liege* **2011**, *80*, 29–41.
30. Crowther, P.A. Physical Properties of Wolf–Rayet Stars. *Annu. Rev. Astron. Astrophys.* **2007**, *45*, 177–219. [[CrossRef](#)]
31. Puls, J.; Vink, J.S.; Najarro, F. Mass loss from hot massive stars. *Astron. Astrophys. Rev.* **2008**, *16*, 209–325. [[CrossRef](#)]
32. Martins, F. Empirical Properties of Very Massive Stars. In *Very Massive Stars in the Local Universe*; Vink, J.S., Ed.; Springer International Publishing: Cham, Switzerland, 2015; Volume 412, pp. 9–42.
33. Walborn, N.R.; Fitzpatrick, E.L. The OB Zoo: A Digital Atlas of Peculiar Spectra. *Publ. Astron. Soc. Pac.* **2000**, *112*, 50–64. [[CrossRef](#)]
34. Snow, T. P., J.; Morton, D.C. Copernicus ultraviolet observations of mass-loss effects in O and B stars. *Astrophys. J. Suppl.* **1976**, *32*, 429–465. [[CrossRef](#)]
35. Snow, T. P., J.; Jenkins, E.B. A catalog of 0.2 Å resolution far-ultraviolet stellar spectra measured with Copernicus. *Astrophys. J. Suppl.* **1977**, *33*, 269–360. [[CrossRef](#)]
36. Walborn, N.R.; Bohlin, R.C. An Atlas of OB Spectra from 1000Å to 1200Å. *Publ. Astron. Soc. Pac.* **1996**, *108*, 477. [[CrossRef](#)]
37. Walborn, N.R.; Nichols-Bohlin, J.; Panek, R.J. International Ultraviolet Explorer Atlas of O-Type Spectra from 1200 to 1900 Å. NASA Ref. Publ.; 1985; 1155. Available online: <https://ui.adsabs.harvard.edu/abs/1995NASRP1363.....W/abstract> (accessed on 12 August 2020).
38. Walborn, N.R.; Parker, J.W.; Nichols, J.S. International Ultraviolet Explorer Atlas of B-Type Spectra from 1200 to 1900 Å. NASA Ref. Publ.; 1995; 1363. Available online: <https://ui.adsabs.harvard.edu/abs/1985NASRP1155.....W/abstract> (accessed on 12 August 2020).
39. Walborn, N.R.; Nichols-Bohlin, J. Ultraviolet spectral morphology of the O stars. IV. The OB supergiant sequence. *Publ. Astron. Soc. Pac.* **1987**, *99*, 40–53. [[CrossRef](#)]
40. Pellerin, A.; Fullerton, A.W.; Robert, C.; Howk, J.C.; Hutchings, J.B.; Walborn, N.R.; Bianchi, L.; Crowther, P.A.; Sonneborn, G. An Atlas of Galactic OB Spectra Observed with the Far Ultraviolet Spectroscopic Explorer. *Astrophys. J. Suppl.* **2002**, *143*, 159–200. [[CrossRef](#)]

41. Walborn, N.R.; Fullerton, A.W.; Crowther, P.A.; Bianchi, L.; Hutchings, J.B.; Pellerin, A.; Sonneborn, G.; Willis, A.J. Far Ultraviolet Spectroscopic Explorer Atlas of OB Stars in the Magellanic Clouds. *Astrophys. J. Suppl.* **2002**, *141*, 443–468. [[CrossRef](#)]
42. Crowther, P.A.; Hillier, D.J.; Evans, C.J.; Fullerton, A.W.; De Marco, O.; Willis, A.J. Revised Stellar Temperatures for Magellanic Cloud O Supergiants from Far Ultraviolet Spectroscopic Explorer and Very Large Telescope UV-Visual Echelle Spectrograph Spectroscopy. *Astrophys. J.* **2002**, *579*, 774–799. [[CrossRef](#)]
43. Massa, D.; Fullerton, A.W.; Sonneborn, G.; Hutchings, J.B. Constraints on the Ionization Balance of Hot-Star Winds from FUSE Observations of O Stars in the Large Magellanic Cloud. *Astrophys. J.* **2003**, *586*, 996–1018. [[CrossRef](#)]
44. Fullerton, A.W.; Massa, D.L.; Prinja, R.K. The Discordance of Mass-Loss Estimates for Galactic O-Type Stars. *Astrophys. J.* **2006**, *637*, 1025–1039. [[CrossRef](#)]
45. Walborn, N.R.; Lennon, D.J.; Heap, S.R.; Lindler, D.J.; Smith, L.J.; Evans, C.J.; Parker, J.W. The Ultraviolet and Optical Spectra of Metal-deficient O Stars in the Small Magellanic Cloud. *Publ. Astron. Soc. Pac.* **2000**, *112*, 1243–1261. [[CrossRef](#)]
46. Dean, C.A.; Bruhweiler, F.C. An ultraviolet line list for O star spectra. *Astrophys. J. Suppl.* **1985**, *57*, 133–143. [[CrossRef](#)]
47. Ayres, T.R.; The ASTRAL I & II Science Teams The Advanced Spectral Library (ASTRAL) Project. In *American Astronomical Society Meeting Abstracts*; American Astronomical Society: Washington, DC, USA, 2014; Volume 223, p. 254.37.
48. Willis, A.J.; van der Hucht, K.A.; Conti, P.S.; Garmany, D. An atlas of high resolution IUE ultraviolet spectra of 14 Wolf–Rayet stars. *Astron. Astrophys. Suppl.* **1986**, *63*, 417–599.
49. Schulte-Ladbeck, R.E.; Hillier, D.J.; Herald, J.E. The Hopkins Ultraviolet Telescope Far-Ultraviolet Spectral Atlas of Wolf–Rayet Stars. *Astrophys. J. Lett.* **1995**, *454*, L51. [[CrossRef](#)]
50. Willis, A.J.; Crowther, P.A.; Fullerton, A.W.; Hutchings, J.B.; Sonneborn, G.; Brownsberger, K.; Massa, D.L.; Walborn, N.R. An Atlas of Far-Ultraviolet Spectra of Wolf–Rayet Stars from the FUSE Satellite. *Astrophys. J. Suppl.* **2004**, *154*, 651–672. [[CrossRef](#)]
51. Lucy, L.B.; Solomon, P.M. Mass Loss by Hot Stars. *Astrophys. J.* **1970**, *159*, 879–893. [[CrossRef](#)]
52. Owocki, S.P.; Castor, J.I.; Rybicki, G.B. Time-dependent models of radiatively driven stellar winds. I—Nonlinear evolution of instabilities for a pure absorption model. *Astrophys. J.* **1988**, *335*, 914–930. [[CrossRef](#)]
53. Cantiello, M.; Langer, N.; Brott, I.; de Koter, A.; Shore, S.N.; Vink, J.S.; Voegler, A.; Lennon, D.J.; Yoon, S.C. Sub-surface convection zones in hot massive stars and their observable consequences. *Astron. Astrophys.* **2009**, *499*, 279–290. [[CrossRef](#)]
54. Cantiello, M.; Braithwaite, J.; Brandenburg, A.; Del Sordo, F.; Käpylä, P.; Langer, N. 3D MHD simulations of subsurface convection in OB stars. In *Active OB Stars—Structure, Evolution, Mass Loss, and Critical Limits, IAU Symposium 272*; Neiner, C., Wade, G., Meynet, G., Peters, G., Eds.; Cambridge University Press: New York, NY, USA, 2011; pp. 32–37.
55. Hillier, D.J.; Miller, D.L. Constraints on the Evolution of Massive Stars through Spectral Analysis. I. The WC5 Star HD 165763. *Astrophys. J.* **1999**, *519*, 354–371. [[CrossRef](#)]
56. Sundqvist, J.O.; Puls, J.; Owocki, S.P. Mass loss from inhomogeneous hot star winds. III. An effective-opacity formalism for line radiative transfer in accelerating, clumped two-component media, and first results on theory and diagnostics. *Astron. Astrophys.* **2014**, *568*, A59. [[CrossRef](#)]
57. Owocki, S.P. Dynamical simulation of the “velocity-porosity” reduction in observed strength of stellar wind lines. In *Clumping in Hot-Star Winds*; Hamann, W.R., Feldmeier, A., Oskinova, L.M., Eds.; Universitätsverlag Potsdam: Potsdam, Germany, 2008; pp. 121–124.
58. Owocki, S.P.; Cohen, D.H. The Effect of Porosity on X-ray Emission-Line Profiles from Hot-Star Winds. *Astrophys. J.* **2006**, *648*, 565–571. [[CrossRef](#)]
59. Oskinova, L.M.; Hamann, W.R.; Feldmeier, A. Neglecting the porosity of hot-star winds can lead to underestimating mass-loss rates. *Astron. Astrophys.* **2007**, *476*, 1331–1340. [[CrossRef](#)]
60. Šurlan, B.; Hamann, W.R.; Aret, A.; Kubát, J.; Oskinova, L.M.; Torres, A.F. Macroclumping as solution of the discrepancy between H α and P v mass loss diagnostics for O-type stars. *Astron. Astrophys.* **2013**, *559*, A130. [[CrossRef](#)]
61. Sundqvist, J.O.; Puls, J. Atmospheric NLTE models for the spectroscopic analysis of blue stars with winds. IV. Porosity in physical and velocity space. *Astron. Astrophys.* **2018**, *619*, A59. [[CrossRef](#)]

62. Eversberg, T.; Lépine, S.; Moffat, A.F.J. Outmoving Clumps in the Wind of the Hot O Supergiant ζ Puppis. *Astrophys. J.* **1998**, *494*, 799–805. [[CrossRef](#)]
63. Marchenko, S.V.; Moffat, A.F.J.; Eversberg, T.; Morel, T.; Hill, G.M.; Tovmassian, G.H.; Seggewiss, W. A comprehensive variability study of the enigmatic WN8 stars—Final results. *Mon. Not. R. Astron. Soc.* **1998**, *294*, 642. [[CrossRef](#)]
64. Lépine, S.; Moffat, A.F.J. Wind Inhomogeneities in Wolf–Rayet Stars. II. Investigation of Emission-Line Profile Variations. *Astrophys. J.* **1999**, *514*, 909–931. [[CrossRef](#)]
65. Kaper, L.; Henrichs, H.F.; Nichols, J.S.; Snoek, L.C.; Volten, H.; Zwarthoed, G.A.A. Long- and short-term variability in O-star winds. I. Time series of UV spectra for 10 bright O stars. *Astron. Astrophys. Suppl.* **1996**, *116*, 257–287. [[CrossRef](#)]
66. Snow, T. P., J. Long-term changes in ultraviolet P Cygni profiles observed with Copernicus. *Astrophys. J.* **1977**, *217*, 760–770. [[CrossRef](#)]
67. Massa, D.; Fullerton, A.W.; Nichols, J.S.; Owocki, S.P.; Prinja, R.K.; St-Louis, N.; Willis, A.J.; Altner, B.; Bolton, C.T.; Cassinelli, J.P.; et al. The IUE MEGA Campaign: Wind Variability and Rotation in Early-Type Stars. *Astrophys. J. Lett.* **1995**, *452*, L53. [[CrossRef](#)]
68. Howarth, I.D.; Prinja, R.K.; Massa, D. The IUE MEGA Campaign: The Rotationally Modulated Wind of zeta Puppis. *Astrophys. J. Lett.* **1995**, *452*, L65. [[CrossRef](#)]
69. St-Louis, N.; Dalton, M.J.; Marchenko, S.V.; Moffat, A.F.J.; Willis, A.J. The IUE MEGA Campaign: Wind Structure and Variability of HD 50896 (WN5). *Astrophys. J. Lett.* **1995**, *452*, L57. [[CrossRef](#)]
70. Prinja, R.K.; Massa, D.; Fullerton, A.W. The IUE MEGA Campaign: Modulated Structure in the Wind of HD 64760 (B0.5 Ib). *Astrophys. J. Lett.* **1995**, *452*, L61. [[CrossRef](#)]
71. Berghoefer, T.W.; Baade, D.; Schmitt, J.H.M.M.; Kudritzki, R.P.; Puls, J.; Hillier, D.J.; Pauldrach, A.W.A. Correlated variability in the X-ray and H α emission from the O4If supergiant ζ Puppis. *Astron. Astrophys.* **1996**, *306*, 899.
72. Reid, A.H.N.; Howarth, I.D. Optical time-series spectroscopy of the O4 supergiant ζ Puppis. *Astron. Astrophys.* **1996**, *311*, 616–630.
73. Schmutz, W.; Koenigsberger, G. Long uninterrupted photometric observations of the Wolf–Rayet star EZ CMa by the Toronto BRITE satellite reveal a very fast apsidal motion. *Astron. Astrophys.* **2019**, *624*, L3. [[CrossRef](#)]
74. Koenigsberger, G.; Schmutz, W. The nature of the companion in the Wolf–Rayet system EZ Canis Majoris. *arXiv* **2020**, arXiv:2005.06028.
75. Cassinelli, J.P.; Swank, J.H. X-ray spectra of Orion OB supergiants. *Astrophys. J.* **1983**, *271*, 681–690. [[CrossRef](#)]
76. Cohen, D.H.; Wollman, E.E.; Leutenegger, M.A.; Sundqvist, J.O.; Fullerton, A.W.; Zsargó, J.; Owocki, S.P. Measuring mass-loss rates and constraining shock physics using X-ray line profiles of O stars from the Chandra archive. *Mon. Not. R. Astron. Soc.* **2014**, *439*, 908–923. [[CrossRef](#)]
77. Cardelli, J.A.; Clayton, G.C.; Mathis, J.S. The relationship between infrared, optical, and ultraviolet extinction. *Astrophys. J.* **1989**, *345*, 245–256. [[CrossRef](#)]
78. Schmutz, W. Observations Versus Atmospheric Models of WR Stars (review). In *Wolf–Rayet Stars and Interrelations with Other Massive Stars in Galaxies, IAU Symposium 143*; van der Hucht, K.A.; Hidayat, B., Eds.; Springer: Cham, Switzerland, 1991; pp. 39–52.
79. Lamers, H.J.G.L.M.; Cerruti-Sola, M.; Perinotto, M. The “SEI” Method for Accurate and Efficient Calculations of Line Profiles in Spherically Symmetric Stellar Winds. *Astrophys. J.* **1987**, *314*, 726. [[CrossRef](#)]
80. Hamann, W.R. Line formation in expanding atmospheres: On the validity of the Sobolev approximation. *Astron. Astrophys.* **1981**, *93*, 353–361.
81. Sundqvist, J.O.; Puls, J.; Feldmeier, A. Mass loss from inhomogeneous hot star winds. I. Resonance line formation in 2D models. *Astron. Astrophys.* **2010**, *510*, A11. [[CrossRef](#)]
82. Šurlan, B.; Hamann, W.R.; Kubát, J.; Oskinova, L.M.; Feldmeier, A. Three-dimensional radiative transfer in clumped hot star winds. I. Influence of clumping on the resonance line formation. *Astron. Astrophys.* **2012**, *541*, A37. [[CrossRef](#)]
83. Kurucz, R.L. *Atlas: A Computer Program for Calculating Model Stellar Atmospheres*; SAO Special Report #309; Smithsonian Institution, Astrophysical Observatory: Cambridge, UK, 1970.
84. Kurucz, R.L. Model atmospheres for G, F, A, B, and O stars. *Astrophys. J. Suppl.* **1979**, *40*, 1–340. [[CrossRef](#)]

85. Hubeny, I.; Lanz, T. Non-LTE line-blanketed model atmospheres of hot stars. 1: Hybrid complete linearization/accelerated lambda iteration method. *Astrophys. J.* **1995**, *439*, 875–904. [[CrossRef](#)]
86. Przybilla, N.; Butler, K.; Becker, S.R.; Kudritzki, R.P.; Venn, K.A. Non-LTE line formation for neutral oxygen. Model atom and first results on A-type stars. *Astron. Astrophys.* **2000**, *359*, 1085–1106.
87. Hummer, D.G. The effect of reflected and external radiation on stellar flux distributions. *Astrophys. J.* **1982**, *257*, 724–732. [[CrossRef](#)]
88. Pauldrach, A.W.A.; Hoffmann, T.L.; Lennon, M. Radiation-driven winds of hot luminous stars. XIII. A description of NLTE line blocking and blanketing towards realistic models for expanding atmospheres. *Astron. Astrophys.* **2001**, *375*, 161–195. [[CrossRef](#)]
89. Gräfener, G.; Koesterke, L.; Hamann, W.R. Line-blanketed model atmospheres for WR stars. *Astron. Astrophys.* **2002**, *387*, 244–257. [[CrossRef](#)]
90. Sander, A.; Shenar, T.; Hainich, R.; Gímenez-García, A.; Todt, H.; Hamann, W.R. On the consistent treatment of the quasi-hydrostatic layers in hot star atmospheres. *Astron. Astrophys.* **2015**, *577*, A13. [[CrossRef](#)]
91. Krtićka, J.; Kubát, J. Comoving frame models of hot star winds. II. Reduction of O star wind mass-loss rates in global models. *Astron. Astrophys.* **2017**, *606*, A31. [[CrossRef](#)]
92. Hillier, D.J. WC stars—Hot stars with cold winds. *Astrophys. J.* **1989**, *347*, 392–408. [[CrossRef](#)]
93. Hillier, D.J. An iterative method for the solution of the statistical and radiative equilibrium equations in expanding atmospheres. *Astron. Astrophys.* **1990**, *231*, 116–124.
94. Puls, J.; Urbaneja, M.A.; Venero, R.; Repolust, T.; Springmann, U.; Jokuthy, A.; Mokiem, M.R. Atmospheric NLTE-models for the spectroscopic analysis of blue stars with winds. II. Line-blanketed models. *Astron. Astrophys.* **2005**, *435*, 669–698. [[CrossRef](#)]
95. Carneiro, L.P.; Puls, J.; Hoffmann, T.L.; Holgado, G.; Simón-Díaz, S. Surface abundances of CNO in Galactic O-stars: A pilot study with FASTWIND. *Astron. Astrophys.* **2019**, *623*, A3. [[CrossRef](#)]
96. Puls, J. FASTWIND reloaded: Complete comoving frame transfer for “all” contributing lines. *The Lives and Death-Throes of Massive Stars, IAU Symposium 329*; Eldridge, J.J., Bray, J.C., McClelland, L.A.S., Xiao, L., Eds.; Cambridge University Press: New York, NY, USA, 2017; pp. 435–435.
97. Sander, A.A.C.; Hamann, W.R.; Todt, H.; Hainich, R.; Shenar, T. Coupling hydrodynamics with comoving frame radiative transfer. I. A unified approach for OB and WR stars. *Astron. Astrophys.* **2017**, *603*, A86. [[CrossRef](#)]
98. Sander, A.A.C.; Vink, J.S.; Hamann, W.R. Driving classical Wolf–Rayet winds: A Γ - and Z-dependent mass-loss. *Mon. Not. R. Astron. Soc.* **2020**, *491*, 4406–4425. [[CrossRef](#)]
99. Bouret, J.C.; Lanz, T.; Martins, F.; Marcolino, W.L.F.; Hillier, D.J.; Depagne, E.; Hubeny, I. Massive stars at low metallicity. Evolution and surface abundances of O dwarfs in the SMC. *Astron. Astrophys.* **2013**, *555*, A1. [[CrossRef](#)]
100. Pauldrach, A.W.A.; Kudritzki, R.P.; Puls, J.; Butler, K.; Hunsinger, J. Radiation-driven winds of hot luminous stars. 12: A first step towards detailed UV-line diagnostics of O-stars. *Astron. Astrophys.* **1994**, *283*, 525–560.
101. Pauldrach, A.W.A.; Kudritzki, R.P.; Puls, J.; Butler, K. Radiation driven winds of hot luminous stars. VII—The evolution of massive stars and the morphology of stellar wind spectra. *Astron. Astrophys.* **1990**, *228*, 125–154.
102. Castor, J.I.; Abbott, D.C.; Klein, R.I. Radiation-driven winds in Of stars. *Astrophys. J.* **1975**, *195*, 157–174. [[CrossRef](#)]
103. Pauldrach, A.; Puls, J.; Kudritzki, R.P. Radiation-driven winds of hot luminous stars—Improvements of the theory and first results. *Astron. Astrophys.* **1986**, *164*, 86–100.
104. Gray, D.F. *The Observation and Analysis of Stellar Photospheres*, 2nd ed.; Cambridge University Press: New York, NY, USA, 1992.
105. Hillier, D.J.; Bouret, J.C.; Lanz, T.; Busche, J.R. The influence of rotation on optical emission profiles of O stars. *Mon. Not. R. Astron. Soc.* **2012**, *426*, 1043–1049. [[CrossRef](#)]
106. Bjorkman, J.E.; Cassinelli, J.P. Equatorial disk formation around rotating stars due to Ram pressure confinement by the stellar wind. *Astrophys. J.* **1993**, *409*, 429–449. [[CrossRef](#)]
107. Owocki, S.P.; Cranmer, S.R.; Gayley, K.G. Inhibition FO Wind Compressed Disk Formation by Nonradial Line-Forces in Rotating Hot-Star Winds. *Astrophys. J. Lett.* **1996**, *472*, L115. [[CrossRef](#)]

108. Owocki, S.P.; Gayley, K.G.; Cranmer, S.R. Effects of Gravity Darkening on Radiatively Driven Mass Loss from Rapidly Rotating Stars. In *Boulder-Munich II: Properties of Hot Luminous Stars*; ASP Conf. Ser.; Howarth, I., Ed.; Astronomical Society of the Pacific: San Francisco, CA, USA, 1998; Volume 131, pp. 237–244.
109. Maeder, A. Stellar evolution with rotation IV: Von Zeipel's theorem and anisotropic losses of mass and angular momentum. *Astron. Astrophys.* **1999**, *347*, 185–193.
110. Simon, K.P.; Sturm, E. Disentangling of composite spectra. *Astron. Astrophys.* **1994**, *281*, 286–291.
111. Palate, M.; Rauw, G. Spectral modelling of circular massive binary systems. Towards an understanding of the Struve-Sahade effect? *Astron. Astrophys.* **2012**, *537*, A119. [[CrossRef](#)]
112. Abdul-Masih, M.; Sana, H.; Conroy, K.E.; Sundqvist, J.; Prša, A.; Kochoska, A.; Puls, J. Spectroscopic patch model for massive stars using PHOEBE II and FASTWIND. *Astron. Astrophys.* **2020**, *636*, A59. [[CrossRef](#)]
113. Eaton, J.A.; Cherepashchuk, A.M.; Khaliullin, K.F. Stratification of the Extended Atmosphere of the Wolf–Rayet Component of V444 Cygni. *Astrophys. J.* **1985**, *297*, 266. [[CrossRef](#)]
114. Eaton, J.A.; Cherepashchuk, A.M.; Khaliullin, K.F. Stratification of the Extended Atmosphere of the Wolf–Rayet Component of V444 Cygni: Erratum. *Astrophys. J.* **1988**, *334*, 1076. [[CrossRef](#)]
115. Koenigsberger, G. Spectral variations in WNE Wolf–Rayet binaries: The Fe V + Fe VI pseudo-continuum. *Rev. Mex. Astron. Astrofis.* **1988**, *16*, 75–80.
116. Koenigsberger, G. The Fe V/Fe VI ionization structure in WNE Wolf–Rayet winds. *Astron. Astrophys.* **1990**, *235*, 282.
117. Stevens, I.R.; Blondin, J.M.; Pollock, A.M.T. Colliding Winds from Early-Type Stars in Binary Systems. *Astrophys. J.* **1992**, *386*, 265. [[CrossRef](#)]
118. Stevens, I.R.; Pollock, A.M.T. Stagnation-point flow in colliding-wind binary systems. *Mon. Not. R. Astron. Soc.* **1994**, *269*, 226–234. [[CrossRef](#)]
119. Gayley, K.G.; Owocki, S.P.; Cranmer, S.R. Sudden Radiative Braking in Colliding Hot-Star Winds. *Astrophys. J.* **1997**, *475*, 786–797. [[CrossRef](#)]
120. Luehrs, S. A Colliding-Wind Model for the Wolf–Rayet System HD 152270. *Publ. Astron. Soc. Pac.* **1997**, *109*, 504–513. [[CrossRef](#)]
121. Foellmi, C.; Koenigsberger, G.; Georgiev, L.; Toledano, O.; Marchenko, S.V.; Massey, P.; Dall, T.H.; Moffat, A.F.J.; Morrell, N.; Corcoran, M.; et al. New insights into the nature of the SMC WR/LBV binary HD 5980. *Rev. Mex. De Astron. Y Astrofis.* **2008**, *44*, 3–27.
122. Hillier, D.J.; Koenigsberger, G.; Nazé, Y.; Morrell, N.; Barbá, R.H.; Gamen, R. The enigmatic binary system HD 5980. *Mon. Not. R. Astron. Soc.* **2019**, *486*, 725–742. [[CrossRef](#)]
123. Nielsen, K.E.; Corcoran, M.F.; Gull, T.R.; Hillier, D.J.; Hamaguchi, K.; Ivarsson, S.; Lindler, D.J. η Carinae across the 2003.5 Minimum: Spectroscopic Evidence for Massive Binary Interactions. *Astrophys. J.* **2007**, *660*, 669–686. [[CrossRef](#)]
124. Jerkstrand, A.; Fransson, C.; Kozma, C. The ^{44}Ti -powered spectrum of SN 1987A. *Astron. Astrophys.* **2011**, *530*, A45. [[CrossRef](#)]
125. Ergon, M.; Fransson, C.; Jerkstrand, A.; Kozma, C.; Kromer, M.; Spricer, K. Monte-Carlo methods for NLTE spectral synthesis of supernovae. *Astron. Astrophys.* **2018**, *620*, A156. [[CrossRef](#)]
126. Shingles, L.J.; Sim, S.A.; Kromer, M.; Maguire, K.; Bulla, M.; Collins, C.; Ballance, C.P.; Michel, A.S.; Ramsbottom, C.A.; Röpke, F.K.; et al. Monte Carlo radiative transfer for the nebular phase of Type Ia supernovae. *Mon. Not. R. Astron. Soc.* **2020**, *492*, 2029–2043. [[CrossRef](#)]
127. Long, K.S.; Knigge, C. Modeling the Spectral Signatures of Accretion Disk Winds: A New Monte Carlo Approach. *Astrophys. J.* **2002**, *579*, 725–740. [[CrossRef](#)]
128. Kusterer, D.J.; Nagel, T.; Hartmann, S.; Werner, K.; Feldmeier, A. Monte Carlo radiation transfer in CV disk winds: Application to the AM CVn prototype. *Astron. Astrophys.* **2014**, *561*, A14. [[CrossRef](#)]
129. Parkinson, E.J.; Knigge, C.; Long, K.S.; Matthews, J.H.; Higginbottom, N.; Sim, S.A.; Hewitt, H.A. Accretion disc winds in tidal disruption events: Ultraviolet spectral lines as orientation indicators. *Mon. Not. R. Astron. Soc.* **2020**, *494*, 4914–4929. [[CrossRef](#)]
130. Carciofi, A.C.; Bjorkman, J.E. Non-LTE Monte Carlo Radiative Transfer. I. The Thermal Properties of Keplerian Disks around Classical Be Stars. *Astrophys. J.* **2006**, *639*, 1081–1094. [[CrossRef](#)]
131. Clementel, N.; Madura, T.I.; Kruip, C.J.H.; Icke, V.; Gull, T.R. 3D radiative transfer in η Carinae: Application of the SIMPLEX algorithm to 3D SPH simulations of binary colliding winds. *Mon. Not. R. Astron. Soc.* **2014**, *443*, 2475–2491. [[CrossRef](#)]

132. Clementel, N.; Madura, T.I.; Kruip, C.J.H.; Paardekooper, J.P.; Gull, T.R. 3D radiative transfer simulations of Eta Carinae's inner colliding winds—I. Ionization structure of helium at apastron. *Mon. Not. R. Astron. Soc.* **2015**, *447*, 2445–2458. [[CrossRef](#)]
133. Hillier, D.J.; Lanz, T.; Heap, S.R.; Hubeny, I.; Smith, L.J.; Evans, C.J.; Lennon, D.J.; Bouret, J.C. A Tale of Two Stars: The Extreme O7 Iaf+ Supergiant AV 83 and the OC7.5 III((f)) star AV 69. *Astrophys. J.* **2003**, *588*, 1039–1063. [[CrossRef](#)]
134. Prinja, R.K.; Massa, D.L. Signature of wide-spread clumping in B supergiant winds. *Astron. Astrophys.* **2010**, *521*, L55. [[CrossRef](#)]
135. Prinja, R.K.; Massa, D.L. Ultraviolet diagnostic of porosity-free mass-loss estimates in B stars. *Astron. Astrophys.* **2013**, *559*, A15. [[CrossRef](#)]
136. Cassinelli, J.P.; Cohen, D.H.; Macfarlane, J.J.; Drew, J.E.; Lynas-Gray, A.E.; Hoare, M.G.; Vallergera, J.V.; Welsh, B.Y.; Vedder, P.W.; Hubeny, I.; et al. EUVE Spectroscopy of epsilon Canis Majoris (B2 II) from 70 to 730 Angstrom. *Astrophys. J.* **1995**, *438*, 932. [[CrossRef](#)]
137. Cohen, D.H.; Hurwitz, M.; Cassinelli, J.P.; Bowyer, S. ORFEUS-SPAS II Extreme-Ultraviolet Spectroscopy of epsilon CMa (B2 II). *Astrophys. J. Lett.* **1998**, *500*, L51. [[CrossRef](#)]
138. Najarro, F.; Kudritzki, R.P.; Cassinelli, J.P.; Stahl, O.; Hillier, D.J. Stellar winds and the EUV continuum excess of early B-giants. *Astron. Astrophys.* **1996**, *306*, 892.
139. Cohen, D.H.; Cassinelli, J.P.; Macfarlane, J.J.; Owocki, S.P. EUV/X-ray Emission and the Thermal and Ionization Structure of B Star Winds. In *Thermal and Ionization Aspects of Flows from Hot Stars*; ASP Conf. Ser.; Lamers, H.; Sagar, A., Eds.; Astronomical Society of the Pacific: San Francisco, CA, USA, 2000; Volume 204, pp. 66–78.
140. Kewley, L.J.; Nicholls, D.C.; Sutherland, R.S. Understanding Galaxy Evolution Through Emission Lines. *Annu. Rev. Astron. Astrophys.* **2019**, *57*, 511–570. [[CrossRef](#)]
141. Morisset, C.; Schaerer, D.; Bouret, J.C.; Martins, F. Mid-IR observations of Galactic H II regions: Constraining ionizing spectra of massive stars and the nature of the observed excitation sequences. *Astron. Astrophys.* **2004**, *415*, 577–594. [[CrossRef](#)]
142. Stasińska, G.; Gräfener, G.; Pe na, M.; Hamann, W.R.; Koesterke, L.; Szczerba, R. Comprehensive modelling of the planetary nebula LMC-SMP 61 and its [WC]-type central star. *Astron. Astrophys.* **2004**, *413*, 329–342. [[CrossRef](#)]
143. Morisset, C.; Georgiev, L. A self-consistent stellar and 3D nebular model of planetary nebula IC 418. *Astron. Astrophys.* **2009**, *507*, 1517–1530. [[CrossRef](#)]
144. Danekhar, A.; Todt, H.; Ercolano, B.; Kniazev, A.Y. Observations and three-dimensional photoionization modelling of the Wolf–Rayet planetary nebula Abell 48. *Mon. Not. R. Astron. Soc.* **2014**, *439*, 3605–3615. [[CrossRef](#)]
145. Reyes-Pérez, J.; Morisset, C.; Pe na, M.; Mesa-Delgado, A. A consistent spectral model of WR 136 and its associated bubble NGC 6888. *Mon. Not. R. Astron. Soc.* **2015**, *452*, 1764–1778. [[CrossRef](#)]
146. Walborn, N.R.; Blades, J.C. Spectral Classification of the 30 Doradus Stellar Populations. *Astrophys. J. Suppl.* **1997**, *112*, 457–485. [[CrossRef](#)]
147. Sabín-Sanjulián, C.; Simón-Díaz, S.; Herrero, A.; Walborn, N.R.; Puls, J.; Maíz Apellániz, J.; Evans, C.J.; Brott, I.; de Koter, A.; Garcia, M.; et al. The VLT-FLAMES Tarantula Survey. XIII: On the nature of O Vz stars in 30 Doradus. *Astron. Astrophys.* **2014**, *564*, A39. [[CrossRef](#)]
148. Bouret, J.C.; Lanz, T.; Hillier, D.J.; Heap, S.R.; Hubeny, I.; Lennon, D.J.; Smith, L.J.; Evans, C.J. Quantitative Spectroscopy of O Stars at Low Metallicity: O Dwarfs in NGC 346. *Astrophys. J.* **2003**, *595*, 1182–1205. [[CrossRef](#)]
149. Martins, F.; Schaerer, D.; Hillier, D.J.; Heydari-Malayeri, M. Puzzling wind properties of young massive stars in SMC-N81. *Astron. Astrophys.* **2004**, *420*, 1087–1106. [[CrossRef](#)]
150. Martins, F.; Schaerer, D.; Hillier, D.J.; Meynadier, F.; Heydari-Malayeri, M.; Walborn, N.R. O stars with weak winds: The Galactic case. *Astron. Astrophys.* **2005**, *441*, 735–762. [[CrossRef](#)]
151. de Almeida, E.S.G.; Marcolino, W.L.F.; Bouret, J.C.; Pereira, C.B. Probing the weak wind phenomenon in Galactic O-type giants. *Astron. Astrophys.* **2019**, *628*, A36. [[CrossRef](#)]
152. Oskinova, L.M.; Todt, H.; Ignace, R.; Brown, J.C.; Cassinelli, J.P.; Hamann, W.R. Early magnetic B-type stars: X-ray emission and wind properties. *Mon. Not. R. Astron. Soc.* **2011**, *416*, 1456–1474. [[CrossRef](#)]

153. Muijres, L.E.; Vink, J.S.; de Koter, A.; Müller, P.E.; Langer, N. Predictions for mass-loss rates and terminal wind velocities of massive O-type stars. *Astron. Astrophys.* **2012**, *537*, A37. [[CrossRef](#)]
154. Marcolino, W.L.F.; Bouret, J.C.; Martins, F.; Hillier, D.J.; Lanz, T.; Escolano, C. Analysis of Galactic late-type O dwarfs: More constraints on the weak wind problem. *Astron. Astrophys.* **2009**, *498*, 837–852. [[CrossRef](#)]
155. Cassinelli, J.P.; Olson, G.L. The effects of coronal regions on the X-ray flux and ionization conditions in the winds of OB supergiants and Of stars. *Astrophys. J.* **1979**, *229*, 304–317. [[CrossRef](#)]
156. Bouret, J.C.; Hillier, D.J.; Lanz, T.; Fullerton, A.W. Properties of Galactic early-type O-supergiants. A combined FUV-UV and optical analysis. *Astron. Astrophys.* **2012**, *544*, A67. [[CrossRef](#)]
157. Zsargó, J.; Hillier, D.J.; Bouret, J.C.; Lanz, T.; Leutenegger, M.A.; Cohen, D.H. On the Importance of the Interclump Medium for Superionization: O VI Formation in the Wind of ζ Puppis. *Astrophys. J. Lett.* **2008**, *685*, L149–L152. [[CrossRef](#)]
158. Hearn, A.G. The energy balance and mass loss of stellar coronae. *Astron. Astrophys.* **1975**, *40*, 355–364.
159. Hillier, D.J.; Kudritzki, R.P.; Pauldrach, A.W.; Baade, D.; Cassinelli, J.P.; Puls, J.; Schmitt, J.H.M.M. The 0.1-2.5-KEV X-Ray Spectrum of the O4F-STAR Zeta-Puppis. *Astron. Astrophys.* **1993**, *276*, 117.
160. Cassinelli, J.P.; Miller, N.A.; Waldron, W.L.; MacFarlane, J.J.; Cohen, D.H. Chandra Detection of Doppler-shifted X-Ray Line Profiles from the Wind of ζ Puppis (O4 F). *Astrophys. J. Lett.* **2001**, *554*, L55–L58. [[CrossRef](#)]
161. Chlebowski, T. X-ray emission from O-type stars - Parameters which affect it. *Astrophys. J.* **1989**, *342*, 1091–1107. [[CrossRef](#)]
162. Chlebowski, T.; Garmany, C.D. On winds and X-rays of O-type stars. *Astrophys. J.* **1991**, *368*, 241–251. [[CrossRef](#)]
163. Tramper, F.; Sana, H.; de Koter, A.; Kaper, L. On the Mass-loss Rate of Massive Stars in the Low-metallicity Galaxies IC 1613, WLM, and NGC 3109. *Astrophys. J. Lett.* **2011**, *741*, L8. [[CrossRef](#)]
164. Bouret, J.C.; Lanz, T.; Hillier, D.J.; Martins, F.; Marcolino, W.L.F.; Depagne, E. No breakdown of the radiatively driven wind theory in low-metallicity environments. *Mon. Not. R. Astron. Soc.* **2015**, *449*, 1545–1569. [[CrossRef](#)]
165. Garcia, M.; Herrero, A.; Najarro, F.; Lennon, D.J.; Alejandro Urbaneja, M. Winds of Low-metallicity OB-type Stars: HST-COS Spectroscopy in IC 1613. *Astrophys. J.* **2014**, *788*, 64. [[CrossRef](#)]
166. Vink, J.S.; de Koter, A.; Lamers, H.J.G.L.M. Mass-loss predictions for O and B stars as a function of metallicity. *Astron. Astrophys.* **2001**, *369*, 574–588. [[CrossRef](#)]
167. Lucy, L.B. O-star mass-loss rates at low metallicity. *Astron. Astrophys.* **2012**, *543*, A18. [[CrossRef](#)]
168. Heap, S.R. Stellar Physics in the Primitive Galaxy, I Zw 18. In Proceedings of the IAU General Assembly, Honolulu, HI, USA, 3–14 August 2015; Volume 29, p. 2257699.
169. Garcia, M.; Evans, C.J.; Bestenlehner, J.M.; Bouret, J.C.; Castro, N.; Cervino, M.; Fullerton, A.W.; Gieles, M.; Herrero, A.; de Koter, A.; et al. Massive stars in extremely metal-poor galaxies: A window into the past. *arXiv* **2019**, arXiv:1908.04687.
170. Abbott, D.C. The theory of radiatively driven stellar winds. II. The line acceleration. *Astrophys. J.* **1982**, *259*, 282–301. [[CrossRef](#)]
171. Vink, J.S.; de Koter, A.; Lamers, H.J.G.L.M. On the nature of the bi-stability jump in the winds of early-type supergiants. *Astron. Astrophys.* **1999**, *350*, 181–196.
172. Nugis, T.; Lamers, H.J.G.L.M. The mass-loss rates of Wolf–Rayet stars explained by optically thick radiation driven wind models. *Astron. Astrophys.* **2002**, *389*, 162–179. [[CrossRef](#)]
173. Gräfener, G.; Hamann, W.R. Hydrodynamic model atmospheres for WR stars. Self-consistent modeling of a WC star wind. *Astron. Astrophys.* **2005**, *432*, 633–645. [[CrossRef](#)]
174. Rogers, F.J.; Iglesias, C.A. Radiative Atomic Rosseland Mean Opacity Tables. *Astrophys. J. Suppl.* **1992**, *79*, 507. [[CrossRef](#)]
175. Ishii, M.; Ueno, M.; Kato, M. Core-Halo Structure of a Chemically Homogeneous Massive Star and Bending of the Zero-Age Main Sequence. *PASJ* **1999**, *51*, 417–424. [[CrossRef](#)]
176. Petrovic, J.; Pols, O.; Langer, N. Are luminous and metal-rich Wolf–Rayet stars inflated? *Astron. Astrophys.* **2006**, *450*, 219–225. [[CrossRef](#)]
177. Gräfener, G.; Owocki, S.P.; Vink, J.S. Stellar envelope inflation near the Eddington limit. Implications for the radii of Wolf–Rayet stars and luminous blue variables. *Astron. Astrophys.* **2012**, *538*, A40. [[CrossRef](#)]

178. Grassitelli, L.; Chené, A.N.; Sanyal, D.; Langer, N.; St-Louis, N.; Bestenlehner, J.M.; Fossati, L. Diagnostics of the unstable envelopes of Wolf–Rayet stars. *Astron. Astrophys.* **2016**, *590*, A12. [[CrossRef](#)]
179. Herald, J.E.; Hillier, D.J.; Schulte-Ladbeck, R.E. Tailored Analyses of the WN 8 Stars WR 40 and WR 16. *Astrophys. J.* **2001**, *548*, 932–952. [[CrossRef](#)]
180. Sander, A.; Hamann, W.R.; Todt, H. The Galactic WC stars. Stellar parameters from spectral analyses indicate a new evolutionary sequence. *Astron. Astrophys.* **2012**, *540*, A144. [[CrossRef](#)]
181. Crowther, P.A.; Dessart, L.; Hillier, D.J.; Abbott, J.B.; Fullerton, A.W. Stellar and wind properties of LMC WC4 stars. A metallicity dependence for Wolf–Rayet mass-loss rates. *Astron. Astrophys.* **2002**, *392*, 653–669. [[CrossRef](#)]
182. Hainich, R.; Rühling, U.; Todt, H.; Oskinova, L.M.; Liermann, A.; Gräfener, G.; Foellmi, C.; Schnurr, O.; Hamann, W.R. The Wolf–Rayet stars in the Large Magellanic Cloud. A comprehensive analysis of the WN class. *Astron. Astrophys.* **2014**, *565*, A27. [[CrossRef](#)]
183. Hainich, R.; Pasemann, D.; Todt, H.; Shenar, T.; Sander, A.; Hamann, W.R. Wolf–Rayet stars in the Small Magellanic Cloud. I. Analysis of the single WN stars. *Astron. Astrophys.* **2015**, *581*, A21. [[CrossRef](#)]
184. Neugent, K.F.; Massey, P.; Hillier, D.J.; Morrell, N. The Evolution and Physical Parameters of WN3/O3s: A New Type of Wolf–Rayet Star. *Astrophys. J.* **2017**, *841*, 20. [[CrossRef](#)]
185. Tramper, F.; Gräfener, G.; Hartoog, O.E.; Sana, H.; de Koter, A.; Vink, J.S.; Ellerbroek, L.E.; Langer, N.; Garcia, M.; Kaper, L.; et al. On the nature of WO stars: A quantitative analysis of the WO3 star DR1 in IC 1613. *Astron. Astrophys.* **2013**, *559*, A72. [[CrossRef](#)]
186. Bernat, A.P.; Lambert, D.L. Electron scattering in the expanding atmosphere of P Cygni. *Publ. Astron. Soc. Pac.* **1978**, *90*, 520–525. [[CrossRef](#)]
187. Auer, L.H.; van Blerkom, D. Electron Scattering in Spherically Expanding Envelopes. *Astrophys. J.* **1972**, *178*, 175–181. [[CrossRef](#)]
188. Hillier, D.J. The effects of electron scattering and wind clumping for early emission line stars. *Astron. Astrophys.* **1991**, *247*, 455–468.
189. Najarro, F. Spectroscopy of P Cygni. In *P Cygni 2000: 400 Years of Progress*; ASP Conf. Ser.; de Groot, M.; Sterken, C., Eds.; Astronomical Society of the Pacific: San Francisco, CA, USA, 2001; Volume 233; pp. 133–146.
190. Groh, J.H.; Hillier, D.J.; Damineli, A.; Whitelock, P.A.; Marang, F.; Rossi, C. On the Nature of the Prototype Luminous Blue Variable Ag Carinae. I. Fundamental Parameters During Visual Minimum Phases and Changes in the Bolometric Luminosity During the S-Dor Cycle. *Astrophys. J.* **2009**, *698*, 1698–1720. [[CrossRef](#)]
191. Koenigsberger, G.; Auer, L.H. IUE observations of phase-dependent variations in WN+O systems. *Astrophys. J.* **1985**, *297*, 255–265. [[CrossRef](#)]
192. Neugent, K.F.; Massey, P.; Morrell, N. A Modern Search for Wolf–Rayet Stars in the Magellanic Clouds. IV. A Final Census. *Astrophys. J.* **2018**, *863*, 181. [[CrossRef](#)]
193. Smith, N.; Götzberg, Y.; de Mink, S.E. Extreme isolation of WN3/O3 stars and implications for their evolutionary origin as the elusive stripped binaries. *Mon. Not. R. Astron. Soc.* **2018**, *475*, 772–782. [[CrossRef](#)]
194. Grunhut, J.H.; Wade, G.A.; Neiner, C.; Oksala, M.E.; Petit, V.; Alecian, E.; Bohlender, D.A.; Bouret, J.C.; Henrichs, H.F.; Hussain, G.A.J.; et al. The MiMeS survey of Magnetism in Massive Stars: Magnetic analysis of the O-type stars. *Mon. Not. R. Astron. Soc.* **2017**, *465*, 2432–2470. [[CrossRef](#)]
195. Petit, V.; Wade, G.A.; Schneider, F.R.N.; Fossati, L.; Kamp, K.; Neiner, C.; David-Uraz, A.; Alecian, E.; MiMeS Collaboration. The MiMeS survey of magnetism in massive stars: Magnetic properties of the O-type star population. *Mon. Not. R. Astron. Soc.* **2019**, *489*, 5669–5687. [[CrossRef](#)]
196. Wade, G.A.; Maíz Apellániz, J.; Martins, F.; Petit, V.; Grunhut, J.; Walborn, N.R.; Barbá, R.H.; Gagné, M.; García-Melendo, E.; Jose, J.; et al. NGC 1624-2: A slowly rotating, X-ray luminous Of?p star with an extraordinarily strong magnetic field. *Mon. Not. R. Astron. Soc.* **2012**, *425*, 1278–1293. [[CrossRef](#)]
197. David-Uraz, A.; Erba, C.; Petit, V.; Fullerton, A.W.; Martins, F.; Walborn, N.R.; MacInnis, R.; Barbá, R.H.; Cohen, D.H.; Maíz Apellániz, J.; et al. Extreme resonance line profile variations in the ultraviolet spectra of NGC 1624-2: Probing the giant magnetosphere of the most strongly magnetized known O-type star. *Mon. Not. R. Astron. Soc.* **2019**, *483*, 2814–2824. [[CrossRef](#)]
198. Owocki, S.P.; ud-Doula, A.; Sundqvist, J.O.; Petit, V.; Cohen, D.H.; Townsend, R.H.D. An ‘analytic dynamical magnetosphere’ formalism for X-ray and optical emission from slowly rotating magnetic massive stars. *Mon. Not. R. Astron. Soc.* **2016**, *462*, 3830–3844. [[CrossRef](#)]

199. Martins, F.; Donati, J.F.; Marcolino, W.L.F.; Bouret, J.C.; Wade, G.A.; Escolano, C.; Howarth, I.D.; Mimes Collaboration. Detection of a magnetic field on HD108: Clues to extreme magnetic braking and the Of?p phenomenon. *Mon. Not. R. Astron. Soc.* **2010**, *407*, 1423–1432. [[CrossRef](#)]
200. Marcolino, W.L.F.; Bouret, J.C.; Walborn, N.R.; Howarth, I.D.; Nazé, Y.; Fullerton, A.W.; Wade, G.A.; Hillier, D.J.; Herrero, A. HST/STIS spectroscopy of the magnetic Of?p star HD 108: The low state at ultraviolet wavelengths. *Mon. Not. R. Astron. Soc.* **2012**, *422*, 2314–2321. [[CrossRef](#)]
201. Sundqvist, J.O.; ud-Doula, A.; Owocki, S.P.; Townsend, R.H.D.; Howarth, I.D.; Wade, G.A. A dynamical magnetosphere model for periodic H α emission from the slowly rotating magnetic O star HD 191612. *Mon. Not. R. Astron. Soc.* **2012**, *423*, L21–L25. [[CrossRef](#)]
202. Howarth, I.D.; Walborn, N.R.; Lennon, D.J.; Puls, J.; Nazé, Y.; Annuk, K.; Antokhin, I.; Bohlender, D.; Bond, H.; Donati, J.F.; et al. Towards an understanding of the Of?p star HD 191612: Optical spectroscopy. *Mon. Not. R. Astron. Soc.* **2007**, *381*, 433–446. [[CrossRef](#)]
203. Wade, G.A.; Howarth, I.D.; Townsend, R.H.D.; Grunhut, J.H.; Shultz, M.; Bouret, J.C.; Fullerton, A.; Marcolino, W.; Martins, F.; Nazé, Y.; et al. Confirmation of the magnetic oblique rotator model for the Of?p star HD 191612. *Mon. Not. R. Astron. Soc.* **2011**, *416*, 3160–3169. [[CrossRef](#)]
204. Humphreys, R.M.; Davidson, K. The luminous blue variables: Astrophysical geysers. *Publ. Astron. Soc. Pac.* **1994**, *106*, 1025–1051. [[CrossRef](#)]
205. Najarro, F.; Hillier, D.J.; Stahl, O. A spectroscopic investigation of P Cygni. I. H and HeI lines. *Astron. Astrophys.* **1997**, *326*, 1117–1134.
206. Koenigsberger, G.; Morrell, N.; Hillier, D.J.; Gamen, R.; Schneider, F.R.N.; González-Jiménez, N.; Langer, N.; Barbá, R. The HD 5980 Multiple System: Masses and Evolutionary Status. *Astron. J.* **2014**, *148*, 62. [[CrossRef](#)]
207. Georgiev, L.; Koenigsberger, G.; Hillier, D.J.; Morrell, N.; Barbá, R.; Gamen, R. Wind Structure and Luminosity Variations in the Wolf–Rayet/Luminous Blue Variable HD 5980. *Astron. J.* **2011**, *142*, 191. [[CrossRef](#)]
208. Shenar, T.; Hainich, R.; Todt, H.; Sander, A.; Hamann, W.R.; Moffat, A.F.J.; Eldridge, J.J.; Pablo, H.; Oskinova, L.M.; Richardson, N.D. Wolf–Rayet stars in the Small Magellanic Cloud. II. Analysis of the binaries. *Astron. Astrophys.* **2016**, *591*, A22. [[CrossRef](#)]
209. Sobolev, V.V. *Moving Envelopes of Stars*; Harvard University Press: Cambridge, MA, USA, 1960.
210. Castor, J.I. Spectral line formation in Wolf–Rayet envelopes. *Mon. Not. R. Astron. Soc.* **1970**, *149*, 111. [[CrossRef](#)]
211. Prinja, R.K.; Barlow, M.J.; Howarth, I.D. Terminal velocities for a large sample of O stars, B supergiants, and Wolf–Rayet stars. *Astrophys. J.* **1990**, *361*, 607–620. [[CrossRef](#)]
212. Prinja, R.K.; Barlow, M.J.; Howarth, I.D. Terminal Velocities for a Large Sample of O Stars, B Supergiants, and Wolf–Rayet Stars: Erratum. *Astrophys. J.* **1991**, *383*, 466. [[CrossRef](#)]
213. Howarth, I.D.; Phillips, A.P. The ultraviolet spectrum and interstellar environment of HD 50896. *Mon. Not. R. Astron. Soc.* **1986**, *222*, 809–852. [[CrossRef](#)]
214. Hillier, D.J. An empirical model for the Wolf–Rayet star HD 50896. *Astrophys. J. Suppl.* **1987**, *63*, 965–981. [[CrossRef](#)]
215. Catala, C.; Kunasz, P.B.; Praderie, F. Line formation in the wind of AB Aur. *Astron. Astrophys.* **1984**, *134*, 402–413.
216. Shaviv, N.J. The Porous Atmosphere of η Carinae. *Astrophys. J. Lett.* **2000**, *532*, L137–L140. [[CrossRef](#)] [[PubMed](#)]
217. Shaviv, N.J. The theory of steady-state super-Eddington winds and its application to novae. *Mon. Not. R. Astron. Soc.* **2001**, *326*, 126–146. [[CrossRef](#)]
218. van Marle, A.J.; Owocki, S.P.; Shaviv, N.J. Numerical simulations of continuum-driven winds of super-Eddington stars. *Mon. Not. R. Astron. Soc.* **2008**, *389*, 1353–1359. [[CrossRef](#)]
219. Sander, A.A.C.; Hamann, W.R.; Todt, H.; Hainich, R.; Shenar, T.; Ramachandran, V.; Oskinova, L.M. The Galactic WC and WO stars. The impact of revised distances from Gaia DR2 and their role as massive black hole progenitors. *Astron. Astrophys.* **2019**, *621*, A92. [[CrossRef](#)]
220. Rate, G.; Crowther, P.A. Unlocking Galactic Wolf–Rayet stars with Gaia DR2—I. Distances and absolute magnitudes. *Mon. Not. R. Astron. Soc.* **2020**, *493*, 1512–1529. [[CrossRef](#)]
221. Reimers, D. Circumstellar absorption lines and mass loss from red giants. *Mem. Soc. R. Des Sci. De Liege* **1975**, *8*, 369–382.

222. Nugis, T.; Lamers, H.J.G.L.M. Mass-loss rates of Wolf–Rayet stars as a function of stellar parameters. *Astron. Astrophys.* **2000**, *360*, 227–244.
223. Beasor, E.R.; Davies, B.; Smith, N.; van Loon, J.T.; Gehrz, R.D.; Figer, D.F. A new mass-loss rate prescription for red supergiants. *Mon. Not. R. Astron. Soc.* **2020**, *492*, 5994–6006. [[CrossRef](#)]
224. Paxton, B.; Bildsten, L.; Dotter, A.; Herwig, F.; Lesaffre, P.; Timmes, F. Modules for Experiments in Stellar Astrophysics (MESA). *Astrophys. J. Suppl.* **2011**, *192*, 3. [[CrossRef](#)]
225. Mermilliod, J.C.; Maeder, A. Evolution of massive stars : Comparison of cluster sequences and models with mass loss. *Astron. Astrophys.* **1986**, *158*, 45–49.
226. Smith, N.; Owocki, S.P. On the Role of Continuum-driven Eruptions in the Evolution of Very Massive Stars and Population III Stars. *Astrophys. J. Lett.* **2006**, *645*, L45–L48. [[CrossRef](#)]



© 2020 by the authors. Licensee MDPI, Basel, Switzerland. This article is an open access article distributed under the terms and conditions of the Creative Commons Attribution (CC BY) license (<http://creativecommons.org/licenses/by/4.0/>).